KERNFORSCHUNGSANLAGE JÜLICH GmbH
Institut für Plasmaphysik
Association EURATOM-KFA

Stochastic Field Line Structures Appearing in Field Line Tracing Calculations for a Helical Magnetic Limiter on TORE SUPRA

by

G. Fuchs, B. Steffen, T. Blenski,
A. Grosman and A. Samain

Jül - 1993
Mai 1985
ISSN 0366-0885

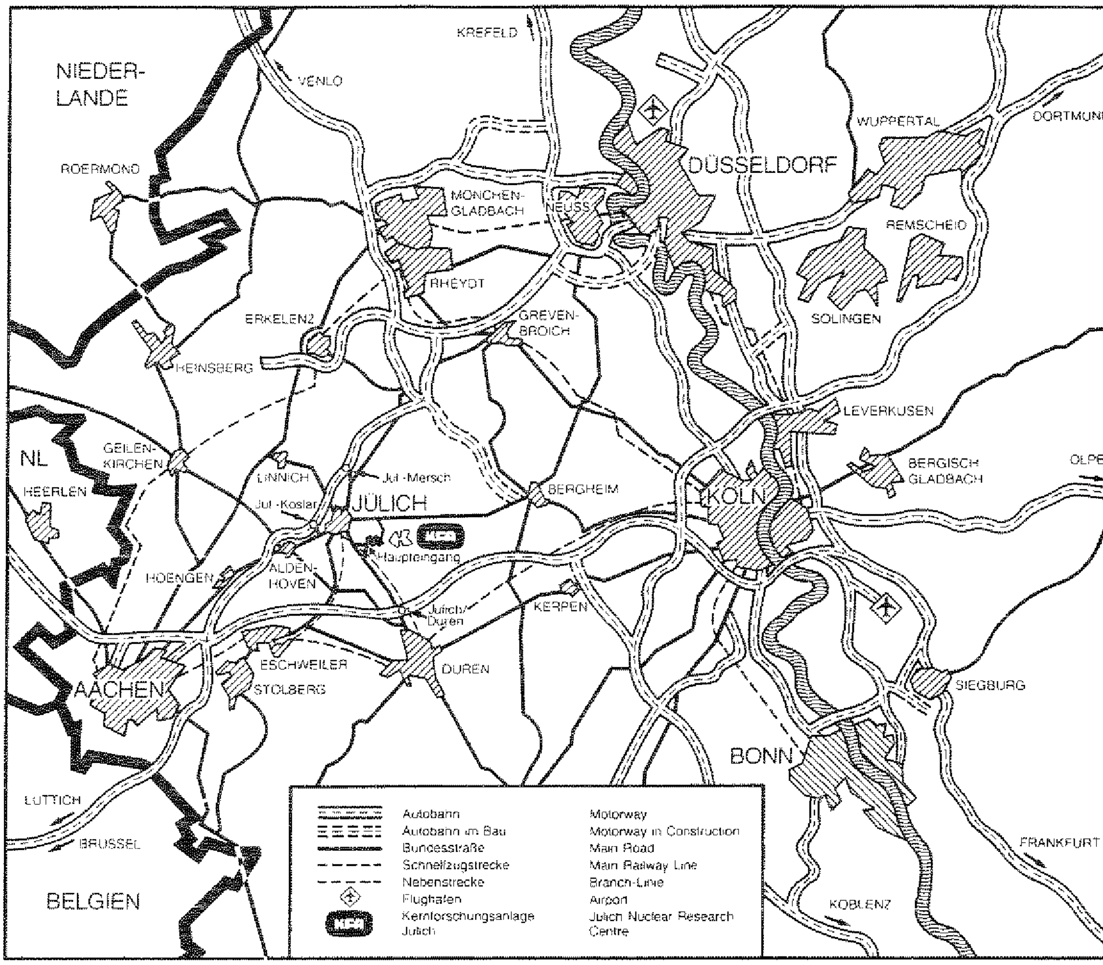

Als Manuskript gedruckt

Berichte der Kernforschungsanlage Jülich – Nr. 1993

Institut für Plasmaphysik, Association EURATOM-KFA Jül - 1993

Zu beziehen durch: ZENTRALBIBLIOTHEK der Kernforschungsanlage Jülich GmbH

Postfach 1913 · D-5170 Jülich (Bundesrepublik Deutschland)

Telefon: 02461/610 · Telex: 833556-0 kf d

Stochastic Field Line Structures Appearing in Field Line Tracing Calculations for a Helical Magnetic Limiter on TORE SUPRA

G. Fuchs and B. Steffen*

Institut für Plasmaphysik ASS-EURATOM-KFA
*Zentralinstitut für Angewandte Mathematik
Kernforschungsanlage Jülich GmbH

T. Blenski[1], A. Grosman and A. Samain

ASS-EURATOM-CEA SUR LA FUSION
Departement de Recherches sur la Fusion Controllee
Centre d'Etudes Nucleaires
Fontenay aux Roses France

---

[1] On leave from the Institute of Nuclear Research Warsav, Poland

CONTENTS

Stochastic Field Line Structures Appearing in Field Line Tracing Calculations for a Helical Magnetic Limiter on TORE SUPRA

G.Fuchs and B.Steffen[*]

Institut für Plasmaphysik ASS-EURATOM-KFA
[*]Zentralinstitut für Angewandte Mathematik
Kernforschungsanlage Jülich GmbH.

T.Blenski[1], *A.Grosman and A.Samain*

ASS-EURATOM-CEA SUR LA FUSION
Departement de Recherches sur la Fusion Controllee
Centre d'Etudes Nucleaires
Fontenay aux Roses France

ABSTRACT

The influence on the structure of the magnetic field of a tokamak produced by small helical currents flowing near the plasma in TORE SUPRA was investigated numerically by drawing Poincaré plots. The current in the helical conductors, the pitch of the windings, the rotational transform and the plasma pressure have been varied. The topology of the magnetic field line structure is discussed in some detail and simple examples are given for illustation.

---

[1] On leave from the Institute of Nuclerar Research Warsav, Poland

1. INTRODUCTION

Helical magnetic multipoles wound resonantly to the magnetic field lines near the boundary of a tokamak have been proposed to form a stochastic boundary [1,2] (usually the term ergodic is used, we will explain the difference below), or a helical divertor [3]. The major advantage of ergodic or stochastic limiters as compared to usual divertors are the low currents required in the conductors (about 1% of the plasma current). The drawback is that the field pattern is sensitive to both the plasma current and pressure.

The stochastic magnetic limiter uses a spectrum of modes, which can be produced with localized perturbation coils [4]. Then, however, a number of magnetic surfaces is destroyed, even where it might not be desirable. Depending on the size of the machine this adverse effect can be reduced by using multipoles of high order. The order is limited by the reqired size of the conductors (limited current density).

The stochastic boundary should give the best results if the mixing of magnetic field lines which takes place on the scale of island diameters (several cm) is combined with the mixing resulting from particle diffusion and heat conduction, acting on a much smaller scale. To combine these two types of processes efficiently reqires a limitation of the island size,i.e a minimum multipole order[5]. The reason is, that the time scale on which mixing is acomplished should match for the two processes, meaning that during the time required for the convective flow to pass - along the long way field lines take - around an island structure the conductive flow should bridge the distance of about an island diameter. These requirements limit the size the islands i.e. call for a high multipole order.

Disturbed magnetic field structures can be rather complicated. To aid the understanding of our results we discuss in some detail the topology of such fields and give a few instructive examples.

2. TOPOLOGY OF MAGNETIC FIELD LINE TRAJECTORIES

Trajectories not crossing each other in a finite region of a n-dimensional space can either be periodic, ergodic or stochastic. In case of ergodic or stochastic trajectories each line is dense in part of the space or on a hyperspace. In the ergodic case the mapping of a cross-section (hyperspace) is continuous along a bundle of trajectories, whereas in the stochastic case it is discontinuous and leads to mixing. The difference can be explained using 2-dimensional regions as examples.

Non-crossing trajectories within a bounded and singly connected 2-dimensional region densly filled with trajectories can be either periodic or they can have a nested set of periodic attractors. Because of $\nabla \cdot B = 0$ the latter case is ruled out for magnetic field lines.

A trajectory on a bounded double connected region as it is the surface of a torus can only be either periodic or ergodic. The torus surface can be cut and rolled flat, in which case the boundary conditions for the trajectory(s) has (have) to be taken periodic. The case is explained in fig.1.

A trajectory on a triple connected region can be periodic, ergodic or stochastic. The stochastic case is explained in fig.2. Take 2 torus surfaces and cut a hole into each (fig.2a). Sewing together the two tori along the cuts results in the structue of fig.2b. It exhibits the topology of two trousers sewed together along the waist band and the ends of the legs. Trajectories are able to pass from one leg to the other. If the surface is cut along the dashed lines of fig.2c, the structure can be rolled flat. The trajectories have now to be taken periodic across the cuts.

There is a simple example to visualize how mixing is obtained in this latter case:

Take a deck of playcards and sort them for black and red. Roll each deck by subsequently moving the top card to the bottom. Join the two decks and continue rolling. Splitting the deck of cards in two half parts will exhibit both colors in each part. Subsequent application of this procedure will finally lead to complete mixing.

Note that the deck of cards stands for a 1-dimensional manifold changing in time; for a fixed time it represents a Poincaré plot of trajectories $x(x_o,t)$.

Mixing a 2-dimensional manifold by following trajectories in a 3-dimensional space is more complicated. An example frequently used in this case is Arnold's cat mapping [6] (see fig.3). Defining a function f(color) on the region A we see that on the transformed region T^2A both, the length of the border between colors and the average gradient ∇f have increased on T^2A as compared to A. Identifying f with a density or a temperature will, together with diffusion and conduction, lead to increased particle or heat transport.

The topology leading to Arnold's cat mapping is found by following magnetic field lines in a tokamak with a bundle divertor, i.e. in the topology of two tori which overlap within a certain volume (see fig.4). In both cases a region is transformed by subsequent application of shear and the displacement of subregions.

To see wether trajectories are ergodic or stochastic in a certain region is done by calculating Liapunov coefficients [7], usually many (>1000) revolutions of the trajectories are required to make this destinction, the smaller the perturbation the more.

3. MAGNETIC ISLANDS

Magnetic islands in a tokamak are structures wich are wound helically onto the torus or in between closed toroidal surfaces. In a tokamak these structures are produced by disturbing the otherwise axissymmetric current distribution by non-symmetric additives. If the disturbing currents follow some of the field lines in parallel, the disturbance is resonant and the currents needed for the distortion are small. Application of different helicities leads to the formation of islands around different surfaces with different rotational transform. Within each island the rotational transform with respect to the main torus is fixed. However, the island itself is usually again composed of different surfaces of different rotational transforms with respect to its magnetic axis. For this reason it may contain subislands just like the original torus. This procedure may carry on.

A hirarchy of (sub)islands will show up in a Poincaré plot as illustrated in fig.5. The difference to mixing of islands having different rotational transform (see below) is that the trajectory stays within the same island chain, although it may jump from one island to another one.

Together with particle diffusion and heat conduction the flow within the hirarchy of islands will lead to a flat distribution of the plasma parameters. The effect of the substructures upon transport is limited by the fact that the lenght along a field line needed to circle around such subislands increases about exponentially with their grade within the hirarchy, whereas at the same time the size becomes exponentially smaller. Therefore the conductive transport will soon smear out the substructures. as far as particle and heat transport is concerned.

A helical perturbance composed of different helical modes will create islands around different resonant surfaces. By increasing the perturbance, the islands with different ι will overlap within a certain volume. The topology of overlapping islands is the same as the one of two interlinked tori (bundle divertor). To see what such a structure looks like when it is placed into a torus, take 2 joint tori (cf.fig.4) and cut them across the planes A, B respectively. Then stretch the 4 tubes and wind them pairwise onto a torus. Thereby each pair is located around the surface with its own rotational transform with respect to the main torus. Finally connect the ends of the pairs.

In fact, depending on the mode numbers m_1, n_1 and m_2, n_2, there might be more than one overlapping volume, however, this does not cause new phaenomena.

Just like in the bundle divertor case the two island strings might both have privat and common flux regions. It is also possible that more than two islands overlap, the resulting geometries may be visualised by adding more islands in fig.4.

Overlapping of islands can be detected in a Poincaré plot if neighbouring trajectories, which had for several revolutions the same rotational transform and lay close together, split after a number of turns *and* exhibit different rotational transform afterwards (cf. fig.6).

4. FIELD LINE TRACING CALCULATIONS FOR TORE SUPRA

4.1. Conductor configuration

The conductor configuration used for the calculations is a slight simplification of a design for TORE SUPRA it is shown in fig.7. Three modules were chosen because TORE SUPRA has a six fold symmetry. The conductors are wound to excite primarily the m = 9, n = 3 mode, they follow trajectories given by

$$\vartheta = \iota \times \phi + \Sigma\, a_i \times \sin(\iota\phi). \qquad (1)$$

a_i can be chosen such that the conductors follow the field lines in parallel. The conducters are placed as close as possible to the plasma, i.e. inside the vacuum system and on the outer side of the torus only. Space is left under the ports on the vacuum vessel. To avoid as far as possible dipole moments in the interior of the plasma, the current in the middle loop is taken twice of these in the other ones. By a proper design the conductors can always be wound in such a way that only one coaxial feed per module is necessary.

4.2. Tokamak field

To obtain the poloidal magnetic field the magnetic flux funktion $\Psi(\beta)$ was calculated in cylindrical coordinates using an eqilibrium code, the result was then aproximated with a spline fit. The magnetic field components were afterwards calculated according

$$B_r = \frac{1}{R} \frac{\partial \Psi}{\partial \vartheta} \qquad B_\vartheta = \frac{1}{R} \frac{\partial \Psi}{\partial R} \qquad (2)$$

Thes values of B were transformed to torus coordinates and then used for the field line tracing calculations.The rotational transform in this field is shown in fig.8 as function of the radius and of its value at the boundary.

5. RESULTS FROM THE FIELD LINE TRACING CALCULATIONS

The results of our calculations for TORE SUPRA are given in the figs.9....21. To obtain them we started field lines from a poloidal plane and traced them around the torus. The starting radii extended from the plasma surface at 82.5 cm to (usually) 60 cm with a step width of 2.5 cm. The start angles were 0.0....0.04; 1.0....1.04; 5.05....5.09 with a step with of 0.01 (for some of the calculations we used 0.0....0.2; .... and a step with of 0.05).

In fig.9 the pattern of start points near $\vartheta = 0$ is seen. Every field line was traced 32 times around the torus. The numerical error grows exponentially with the number of turns, however, for the step width we used it is neglegible up to 100 revolutions around the torus axis. As we pointed out above, the conduction across the field lines will smear out the effect of island structures after several revolutions as far as the plasma density and temperature are concerned. For this reason it is physically not meaningful to follow a field line too far. (see ref.[5])

As we pointed out already perturbed field line structures can be very complicated, for this reason the figs.11...21 are not at all self-explaining, mainly because they do not tell which point is linked to which via how many turns around the torus. This ambiguity could be removed by labeling the points or by using different colors. However, for practical reasons it is impossible to do this for too many points. We have several means to identify how the different points are associated with each other:

We can use a printout of the numerical data

We can watch the points as they appear subsequently on the terminal screen, whereby their appearance is marked with the cursor

We can sort the lines for bundles and plot the throughputs of each bundle for or after a selected number of turns (cf. figs.9 and 10).

The following physical parameters have been varied in the calculations: The current in the conductors, the poloidal β, the rotational transform ι, and the conductor configuration by variation of a_1. (cf. equ.1).

From the figures given in this report and from the more detailed studies, which were performed on the computer graphic terminal we may draw the following cunclusions:

The current in the conductors of the helical multipole (cf. fig.7) should be about 1 kA per Tesla of the main field. Twice this value tends to destroy inner flux surfaces too much and half this value gives too small an effect. (cf. fig.11...13) For the further statements we refer to the value of 1 kA/T.

In all the cases we investigated, several flux surfaces were destroyed, i.e. magnetic islands are found. In most cases this includes the $q = 2$ surface, even in the case of $q \approx 4$ on the plasma boundary.

Overlapping of magnetic islands is - as far as we can tell from the calculations with 32 toroidal revolutions - only occuring in the outermost region ~7 cm from the limiter (at 82.5 cm). Further in we find almost closed flux surfaces in between island chains.

In all the cases we investigated, it took at least 6 turns around the torus axis to bring a field line around an island and then via overlapping into an other one (cf. fig.10).

For larger values of β the mixing of islands in the boundary region is more pronounced. Although we are still able to see some island structure by observing the subsequent appearance of points on the screen, this structure is obscured in the final picture.

With increasing β the island structures around the different rational q - surfaces exhibit larger mode numbers or indicate the presence of several modes (m/n = const.).

Although the destruction of surfaces in the boundary region is more easily obtained for $q \simeq 3$, it is also found for other values. This is true even in the case when the $q = 3$ surface is outside the plasma region. The disturbing field needed to give island overlapping in such a case is not markedly larger as compared to the case when the $q = 3$ surface is present (about a factor 1.5...2). Apparently the coil configuration of fig.7 has a rather large Fourier component for $m = 7$ $n = 3$ which is able to cause ergodization if $q(a) < 3$ in the boundary.

APPENDIX A: A SIMULATION OF RADIAL TRANSPORT IN STOCHASTIC FIELDS

To simulate the combined transport resulting from a stochastic magnetic field *and* conduction we added a pure radial field to a perdurbing helical field. Note, this field is not divergence free just as it is required for a radial outflux.

First we need to know the location of the last closed flux surface. To find it, we made a Poincare plot for a case without the radial contribution and found the intersection of the last closed flux surface with a poloidal plane by inspection on a terminal screen. The inersection points were approximated by a curve which is obtained using a spline fit. Then we started field lines equally spaced on the curve and traced them around the torus, whereby we produced 100 surface elements (of different area).On this last closed flux surface we distributed with constant density 10^4 points and taraced them in the field with the radial additive until they crossed a prescibed toroidal suface. Finally we calculated the density of these intersection points on the outer surface.

For the calculations we used a radial perturbation field composed of pure helical modes ($B_r \propto \sin(m\vartheta - n\phi)$), because otherwise the programme would have run by far too long on the computer. Because these calculations have been done for TEXTOR, where we considered a mixing of islands around $q = 4$, we took the cases of a pure $m = 4$, $n = 1$ mode and an equal mixe between $m = 4$ and $m = 5$ with $n = 1$, the result will be qulitatively the same for TORE SUPRA and for other mode numbers.

The results for the two above cases are shown in the figs.22 and 23 and can be summarized as follows:

> The density of first intersection points with a toroidal surface is in both cases not constant.
>
> The variation in the denisty is even larger for the case of mode mixing.

The field lines are more likely to hit the surface on the inner side of the torus first.

From this finding we may draw the following conclusions:

The loading to a surface or to limiters caused by an stochastic plasma boundary needs not be uniform.

The limiter configuration should be adapted to the magnetic field configuration. Helically or partly helically wound limiters would be most adequate.

In contrary to what is sometimes claimed in the literature the advantage of the stochastic stucture is not an equal loading of the torus surface it is instead the fact that magnetic field lines in front of the limiter are linked to that limiter, allowing for rapid recycling and therefore for a cold plasma in this region.

APPENDIX B:CALCULATIONS FOR SHORTER COILS.

The engineering study which was done in parallel to our calculations suggests to use shorter coils, because they are easier to implement into the machine. The conductor paths of such coils are indicated in fig.24. Our computer programm was capable of calculating Poincaré plots for this case, they are shown in the figs.25 and 26 for two different values of the rotational transform.

As expected, the current in the conductors has to be increased by about the same ratio by which the covered area was reduced in order to achieve the same width of the ergodized boundary layer. The currents used in the figs.24.and 25 may be somewhat reduced (30%) without loss of ergodicity in the boundary zone allowing to reduce the destruction of inner flux surfaces.

The mayor difference between the two coil configurations which have been investigated seems to be that for the shorter coils the islands with mode numbers m = 5; n = 3 are significantly larger.

ACKNOWLEDGEMENT

The authors thank P.Börner for the help with the computer and A.Kaleck for providing us with the equilibrium flux functions.

REFERENCES

[1] W.Engelhardt and W.Feneberg; J.Nucl Mat.**76&77**, 518 (1978)

[2] Feneberg and G.H.Wolf; Nucl. Fus. **21**, 669 (1981)

[3] F.Karger and K.Lackner; Phys. Lett. **61A**, 385 (1977)

[4] H.Belitz, K.H.Dippel and G.H.Wolf; EURATOM Tokamak Workshop Schliersee 8 - 10 Nov. (1982)

[5] G.Fuchs, A.Nicolai, G.H.Wolf and B.Steffen; Jül. Report 1820 (1982)

[6] V.I.Arnold and A.Avez; Ergodic Problems in Classical Mechanics, Benjamin, New York (1968)

[7] A.J.Lichtenberg and M.A.Liebermann; Regular and Stochastic Motion, Appl.Math. Sci. **38** Chap.5, Springer (1983) and literature referenced therein.

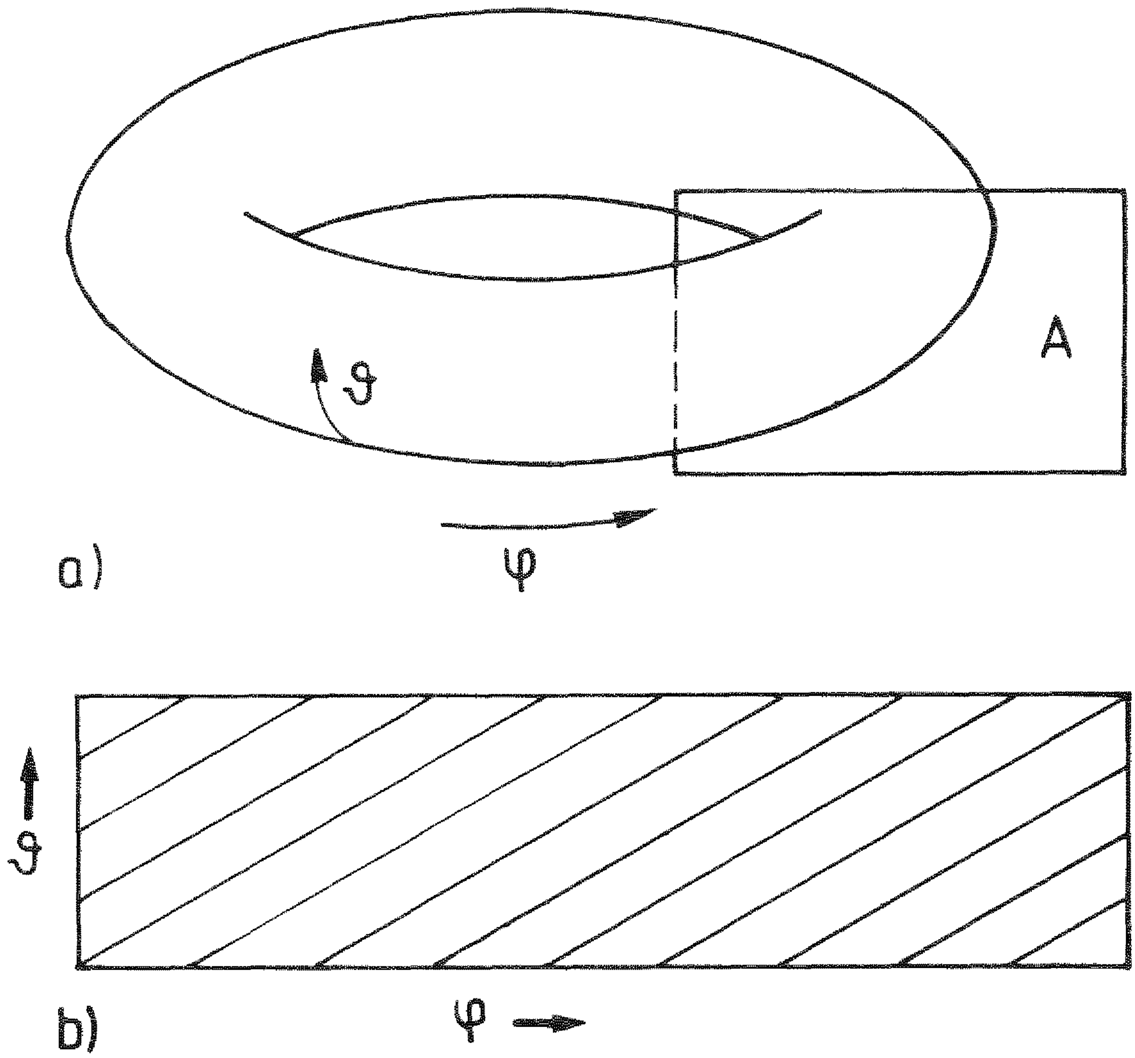

Fig. 1 Toroidal surface cut twice and rolled flat. The boundary conditions are to be taken periodic on the flat surface. The trajectory(s) can be either periodic or ergodic.

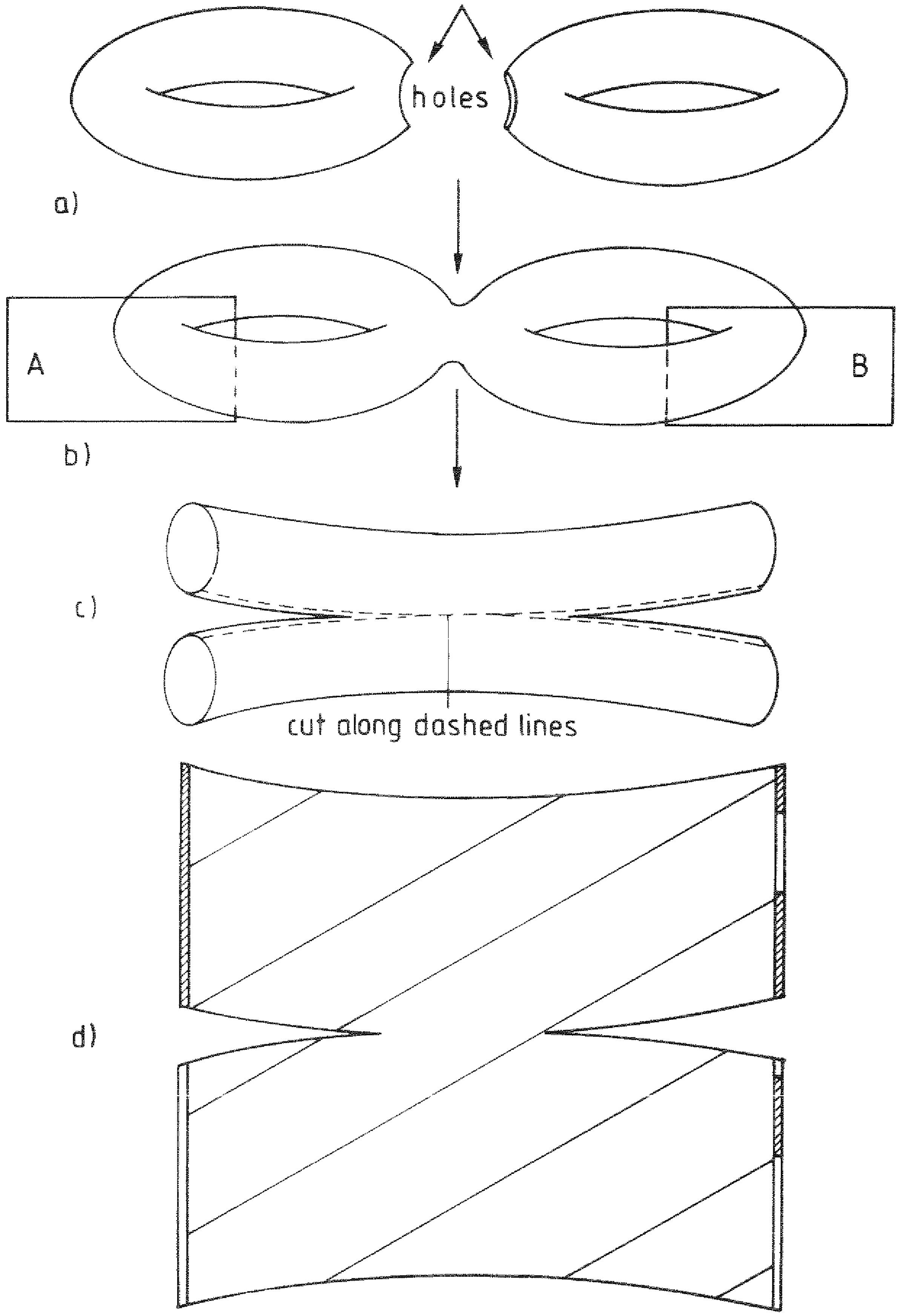

Fig. 2 a) Torus surface with a hole.

b) Two torus surfaces with holes joint together.

c) Two joint torus surfaces cut across the planes A and B in 'b'.

d) Structure cut along the dashed lines in 'c' and rolled flat. Field lines of uniform color (black or white) on the two left entrances are mixed in the right exits.

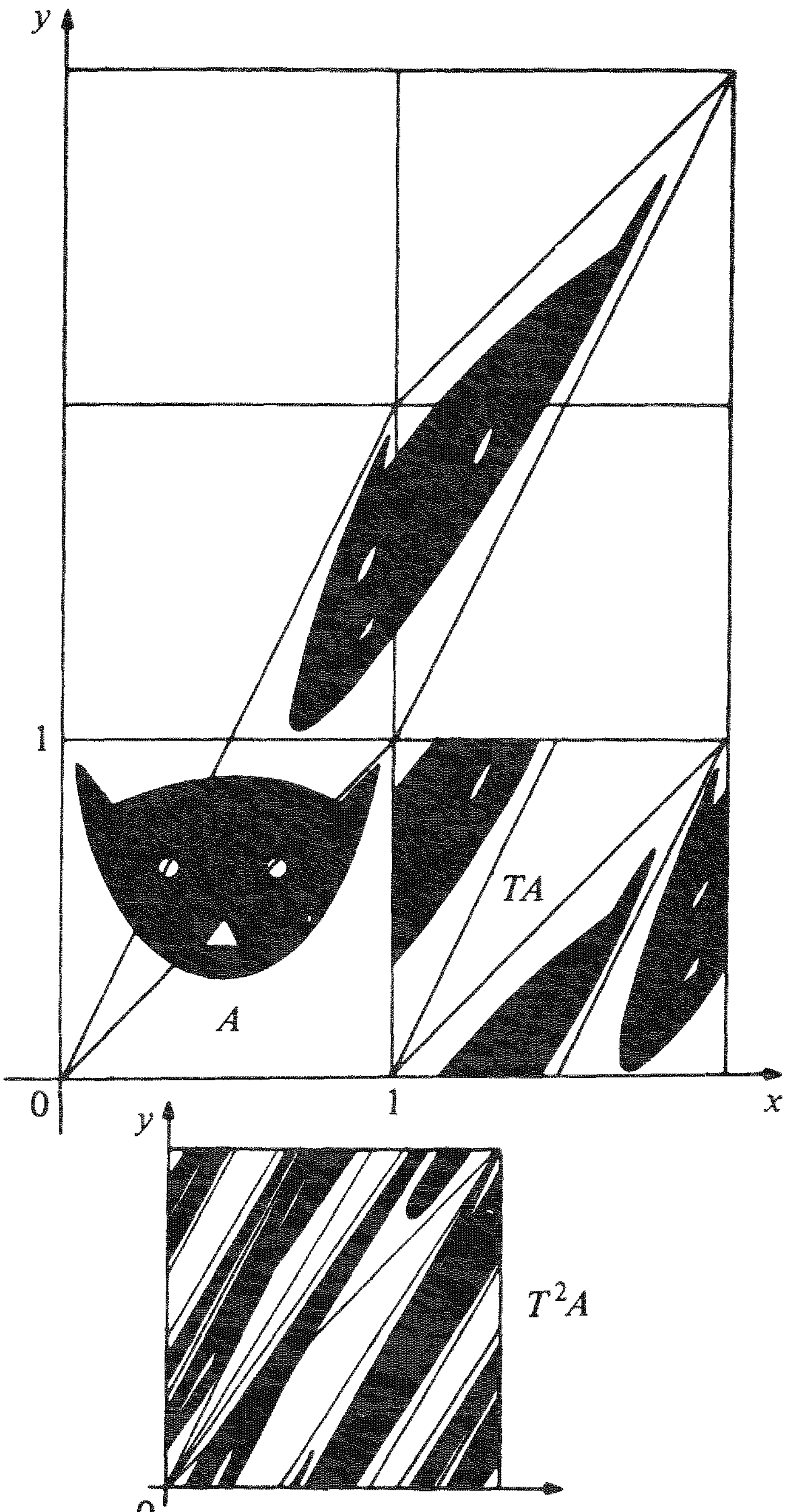

Fig. 3 Arnold's cat mapping, after [6]

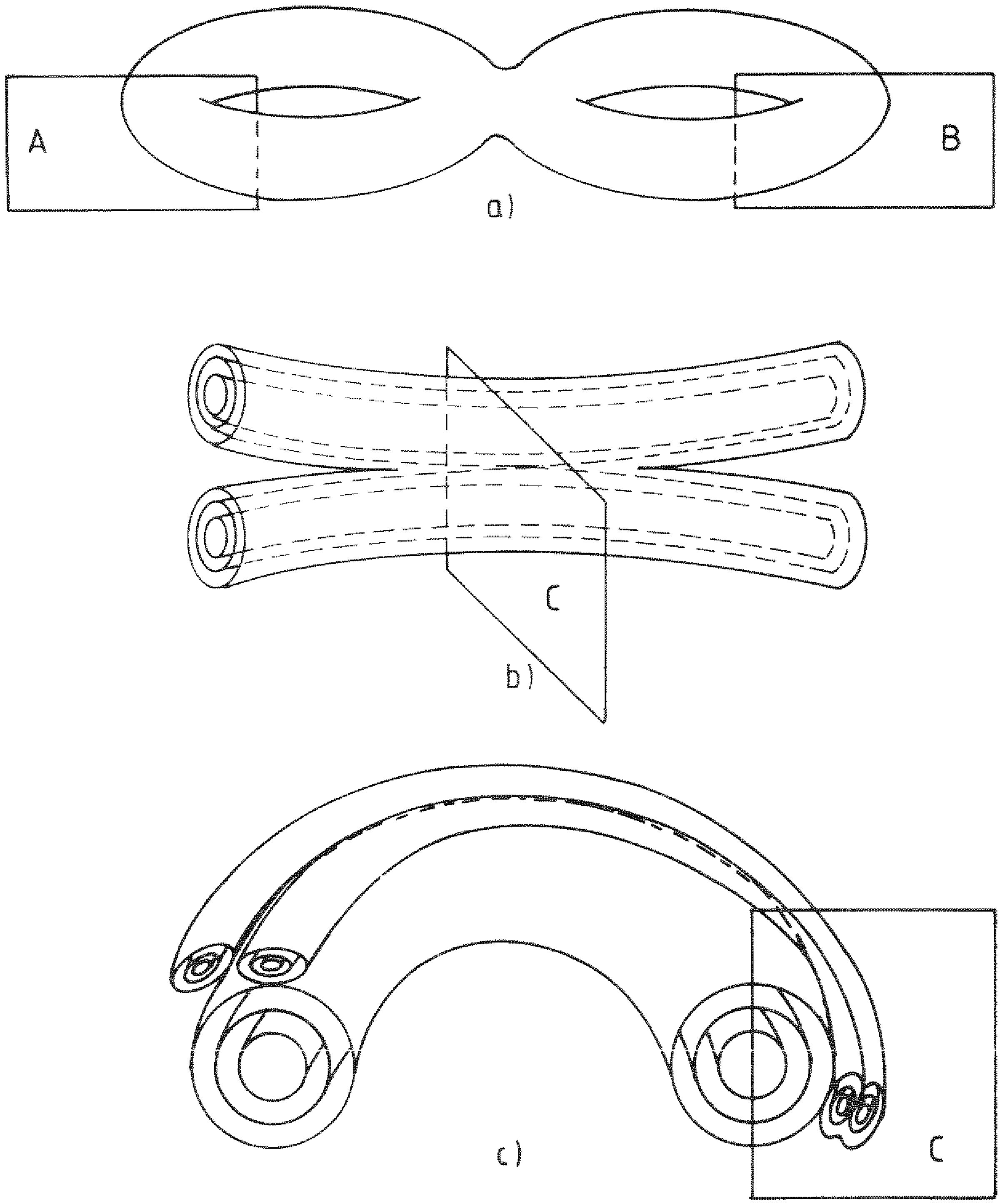

Fig. 4 a) Two overlapping tori (bundle divertor).

b) The configuration of 'a' cut aross the planes A and B, exhibiting a privat- and a common flux surface and the separatrix in between.

c) The structure of 'b' wound as two interlinking island structures onto a torus. To keep the figure simple,the structures which would result by following the islands further around the torus are omitted.

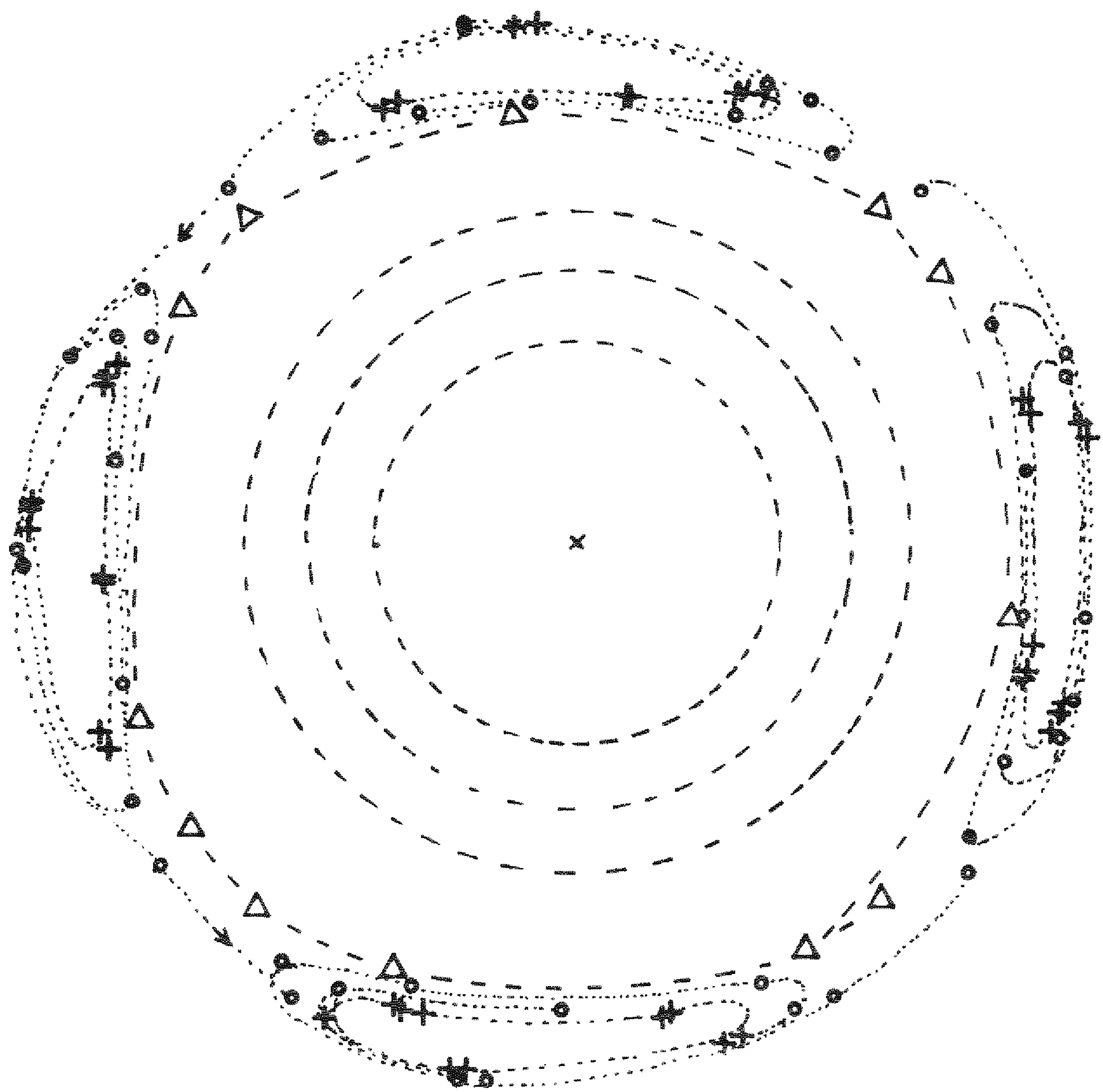

Fig. 5 The appearance of islands containing sub islands on a Poincaré plot. Three trajectories have been started at different radii. The one marked by Δ is on a closed flux surface, the one marked by + stays within the island and the one marked by o indicates a sub-island structure. The fact that the latter trajectory jumps from one island to the next indicates that the island has on its rim the topology indicated in fig.2.

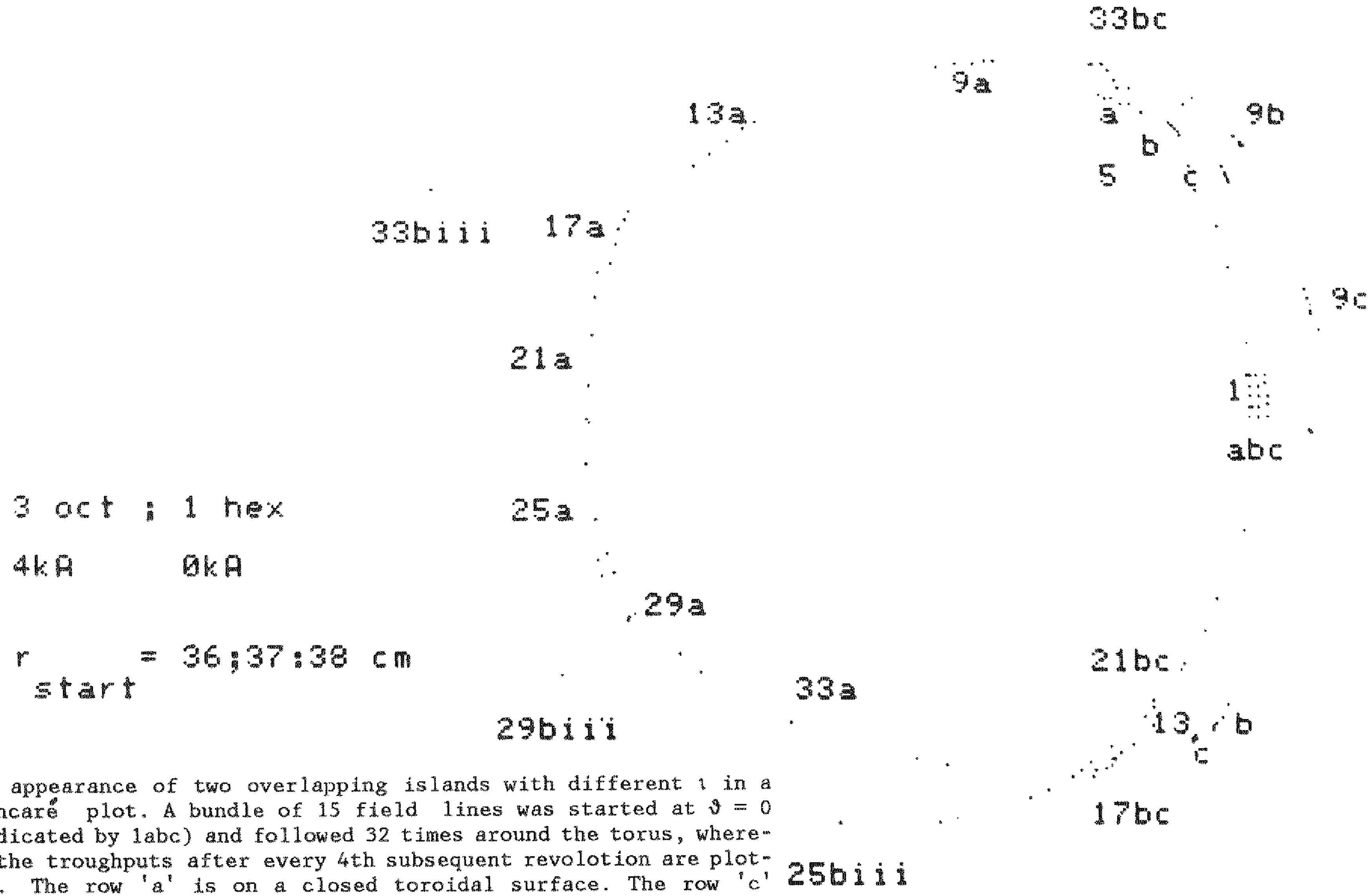

Fig. 6 The appearance of two overlapping islands with different ι in a Poincaré plot. A bundle of 15 field lines was started at $\vartheta = 0$ (indicated by 1abc) and followed 32 times around the torus, whereby the troughputs after every 4th subsequent revolotion are plotted. The row 'a' is on a closed toroidal surface. The row 'c' stays within the q = 4 island. In the row 'b' the middle point is lost from the island after 1 turn around the island's magnetic axis as seen on 25,29,33biii.

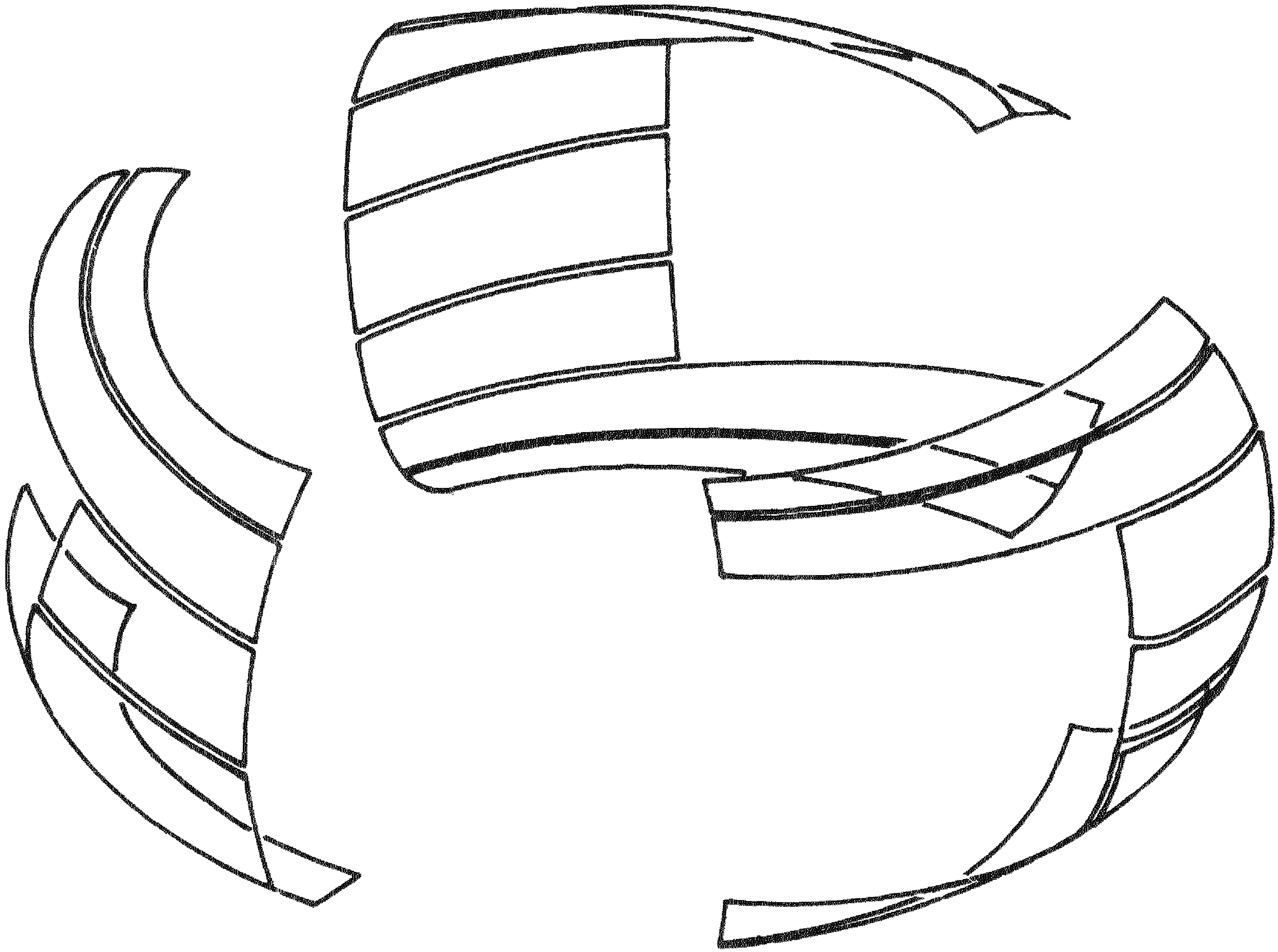

Fig. 7 Conductor configuration used for TORE SUPRA.

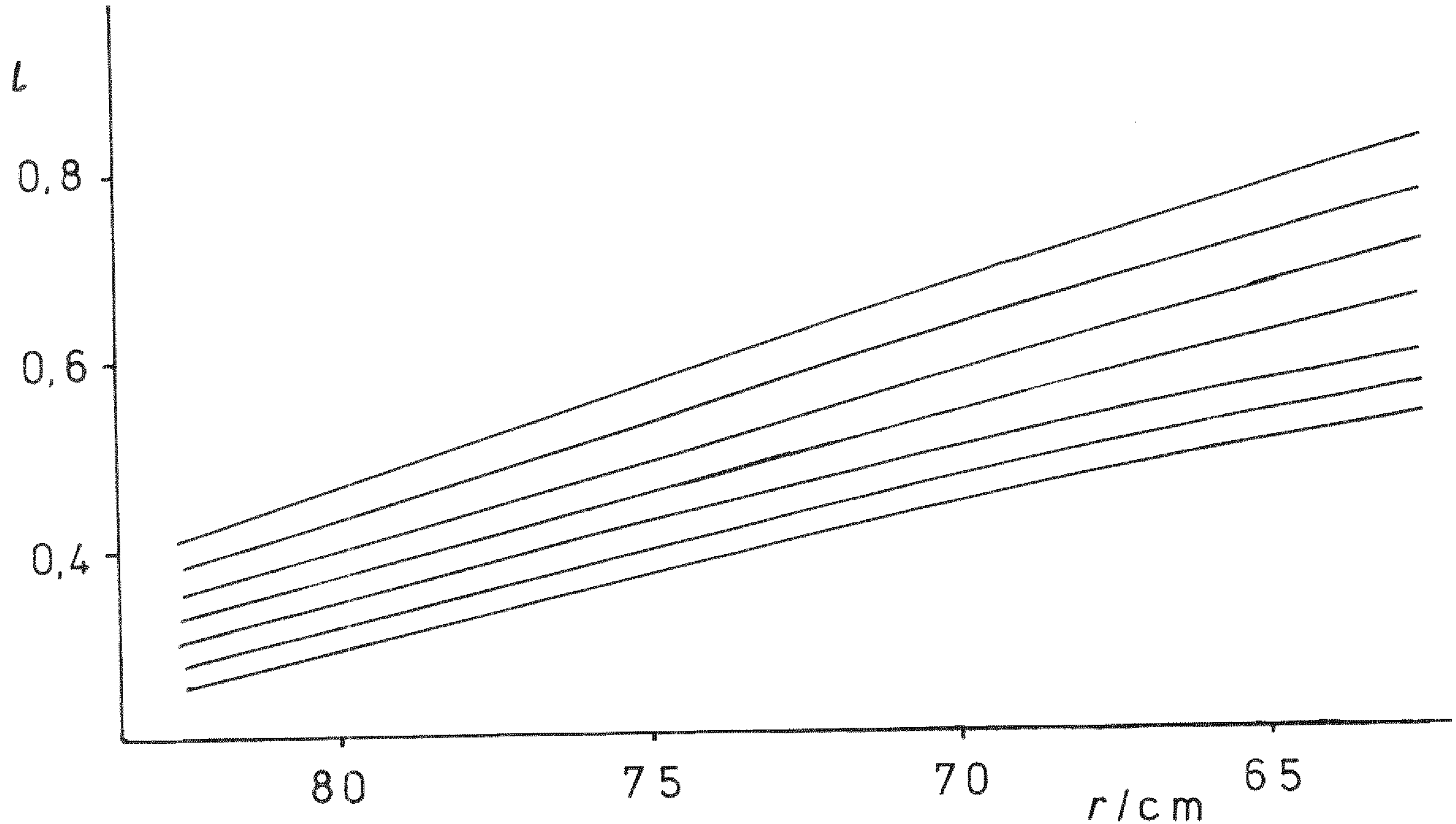

Fig.8 $\iota(r)$ for $\beta = 1$ and $\vartheta = 0$. The parameter is $\iota(a)$, whereby a = 65cm.

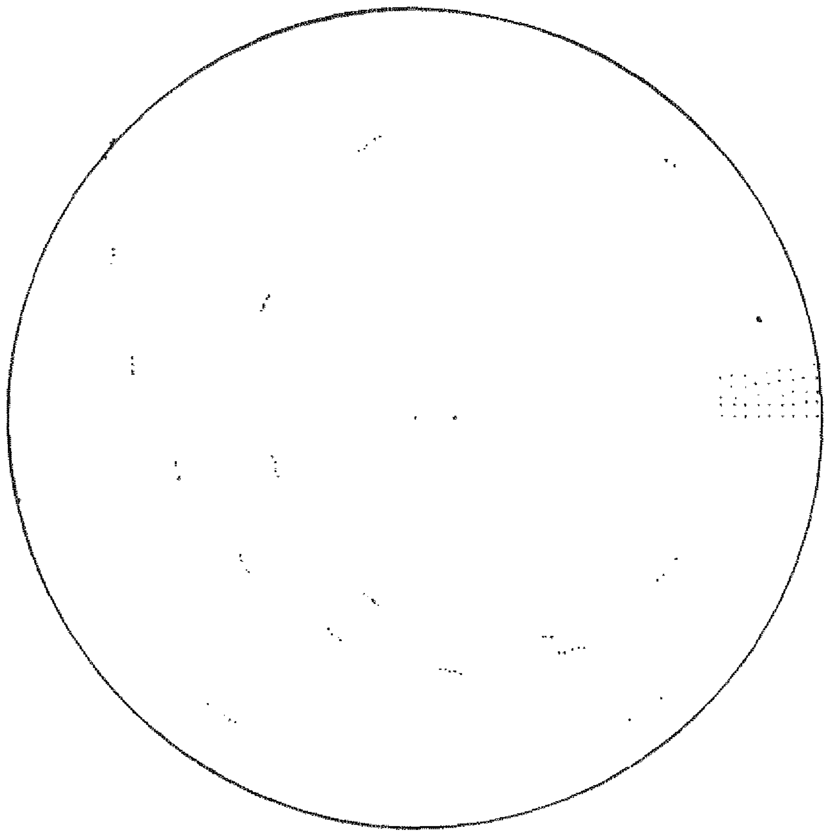

$\beta_p = 2$

$\iota(a) = 0{,}276$

$\frac{I_{hel}}{B_\varphi} = 1 \; \frac{kA}{T}$

$a_1 = 0{,}46$

Fig. 9 A bundle of magnetic field lines started from different radii (62.5 cm .... 80.5 cm step 2.5 cm) and angles traced twize around the torus.

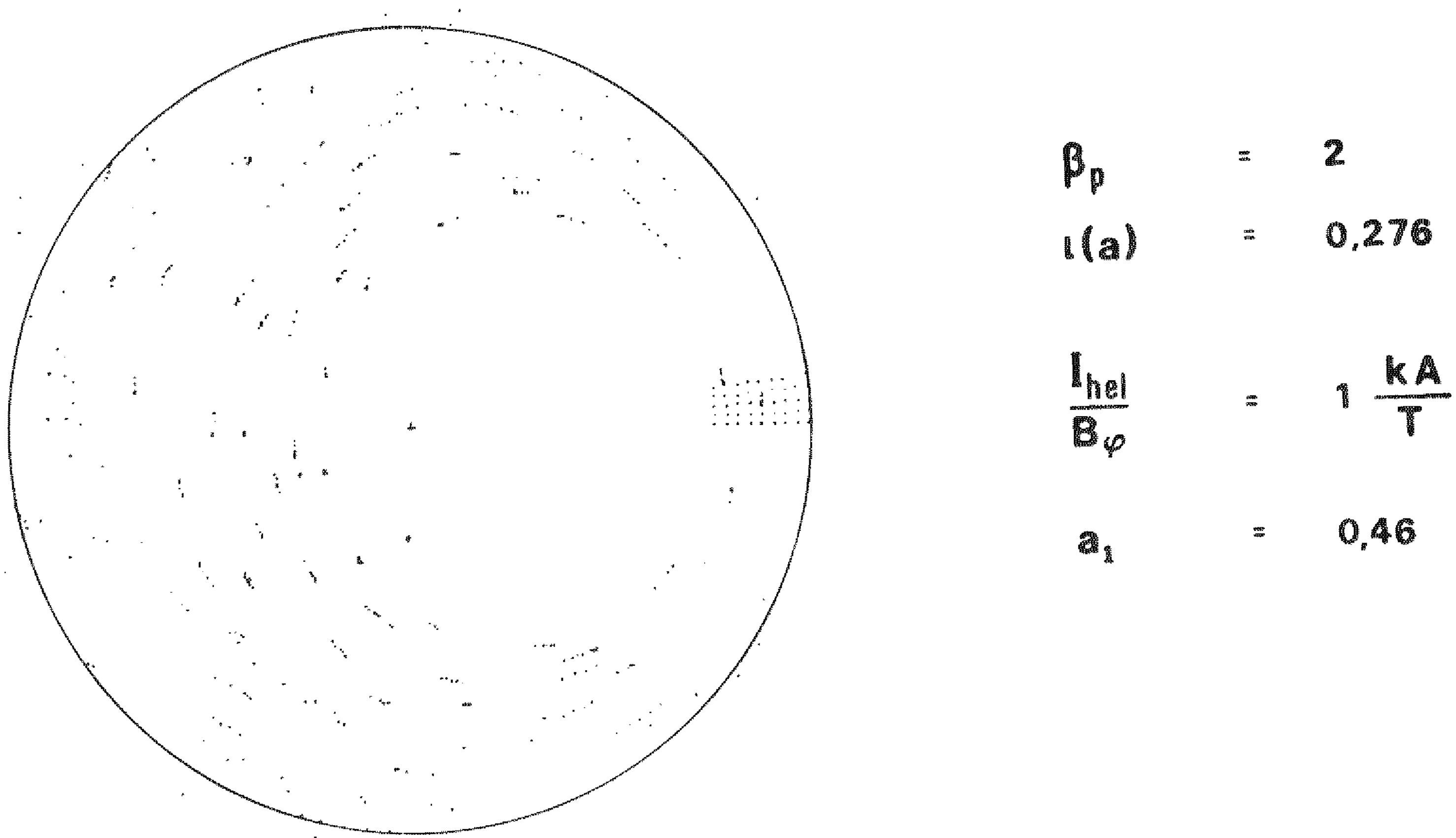

Fig. 10 The same bundle as fig.8 traced 10 times around the torus. The onset of mixing is discovered for the field lines started near the boundary (cf.fig.6).

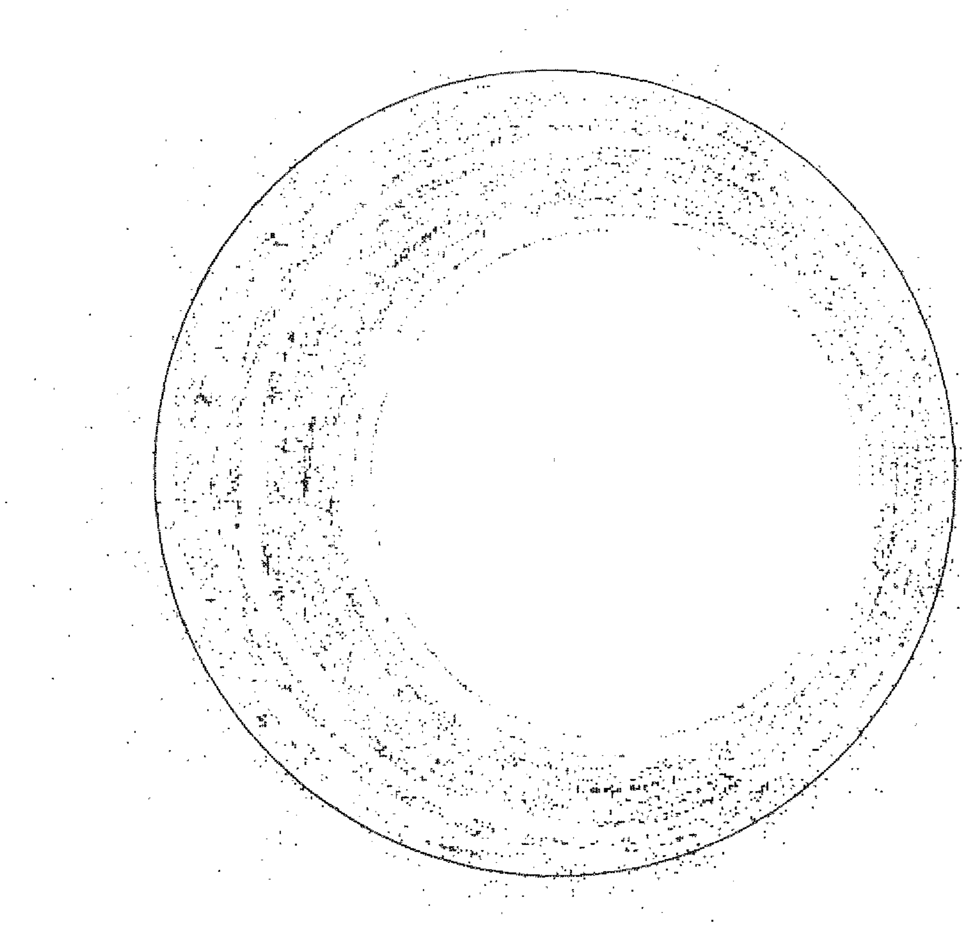

β = 1

$\iota(a)$ = 0,33

I_{hel}/B_{φ} = 0,5 kA / T

a_1 = 0,36

Fig. 11 Poincaré plot for a weak disturbance, which is not sufficient to cause ergodization in the boundary layer. The current in the disturbing coils is normalized to the main magnetic field.

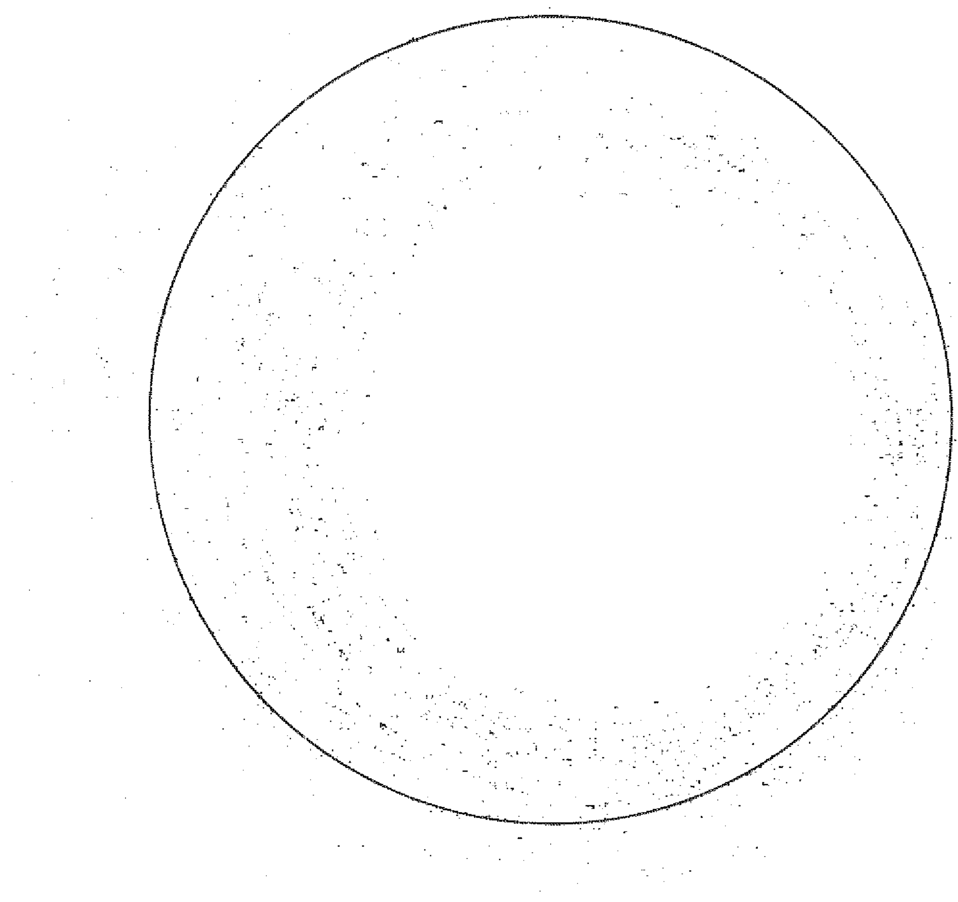

$\beta = 1$

$\iota(a) = 0{,}33$

$I_{hel}/B_\varphi = 1$ kA / T

$a_1 = 0{,}36$

Fig.12 Poincaré plot for a disturbance twize as large as in fig.11. The ergodized zone in the boundary is about 7cm wide, which is just right. Although this claim is not evident from the figure, it becomes clear when one watches the subsequent appearance of the field line intersection points on the terminale screen.

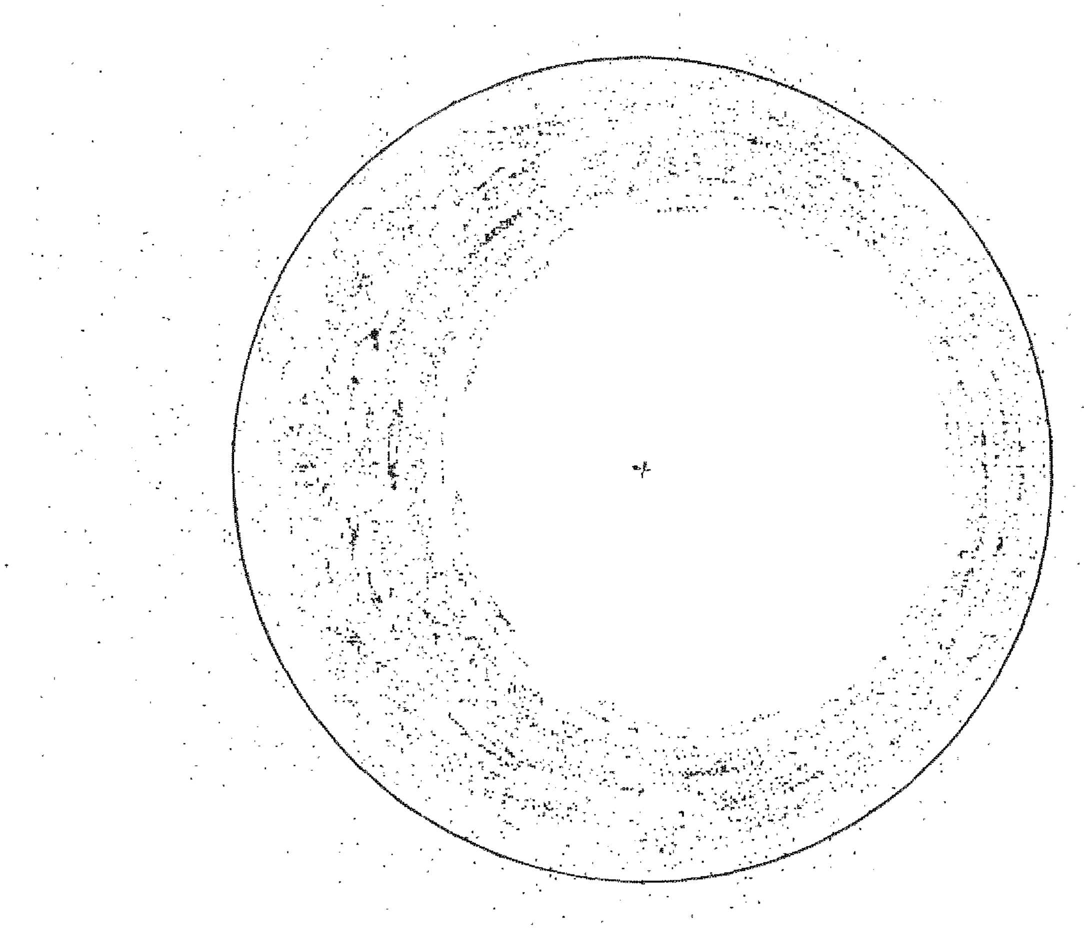

$$\beta_{pol} = 1$$

$$\iota(a) = 0{,}33$$

$$\frac{I_{hel}}{B_\varphi} = 2\,\frac{kA}{T}$$

$$a_1 = 0{,}36$$

Fig. 13 The disturbance is twize the one as in fig.12. The points to the left are in a region where the poloidal field is not declared in our model, they are meaningless.

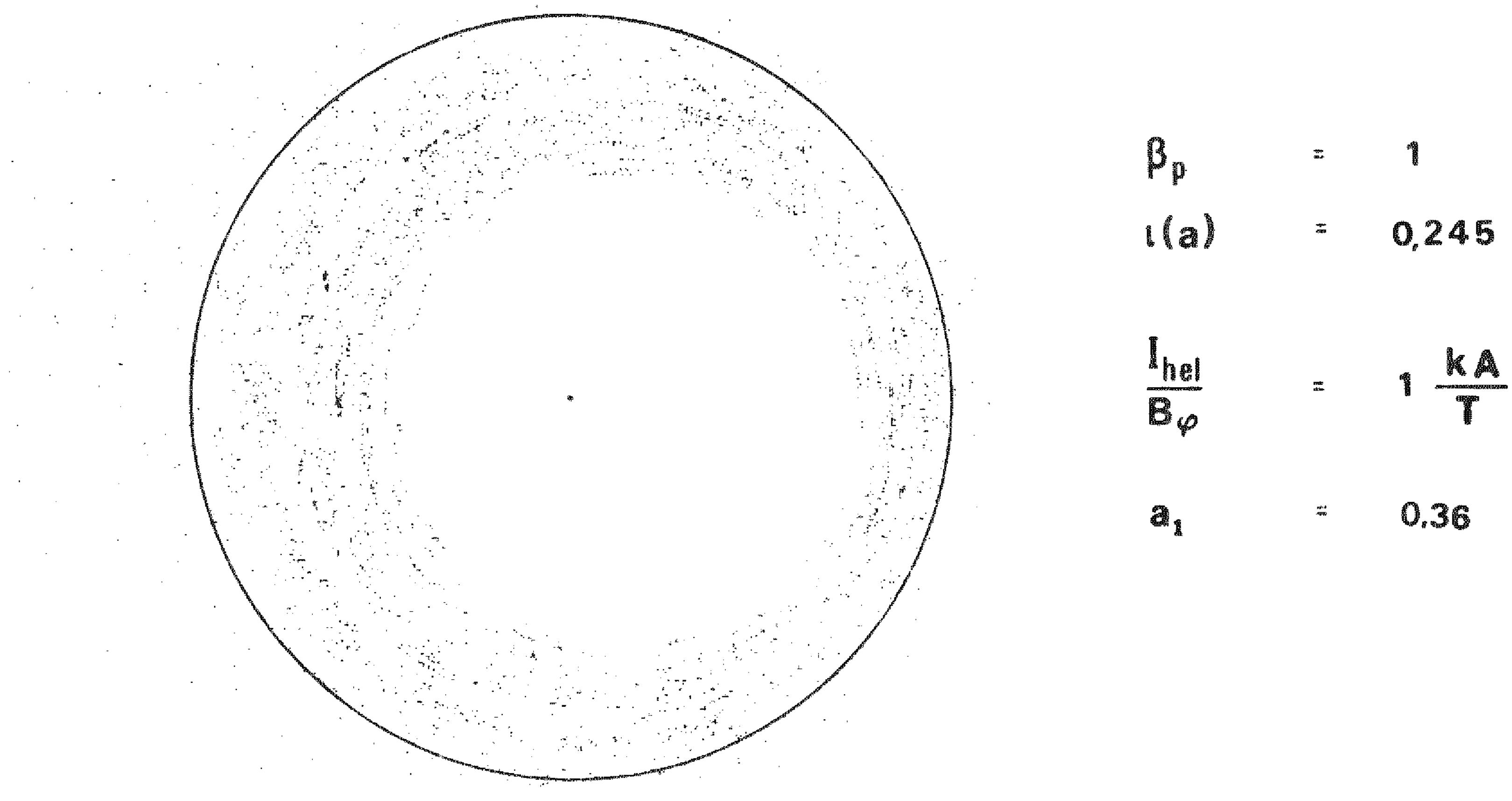

Fig. 14 Island structures are more pronounced in the case of low β and low ι. This case shows 6/2 and 7/2 island structures.

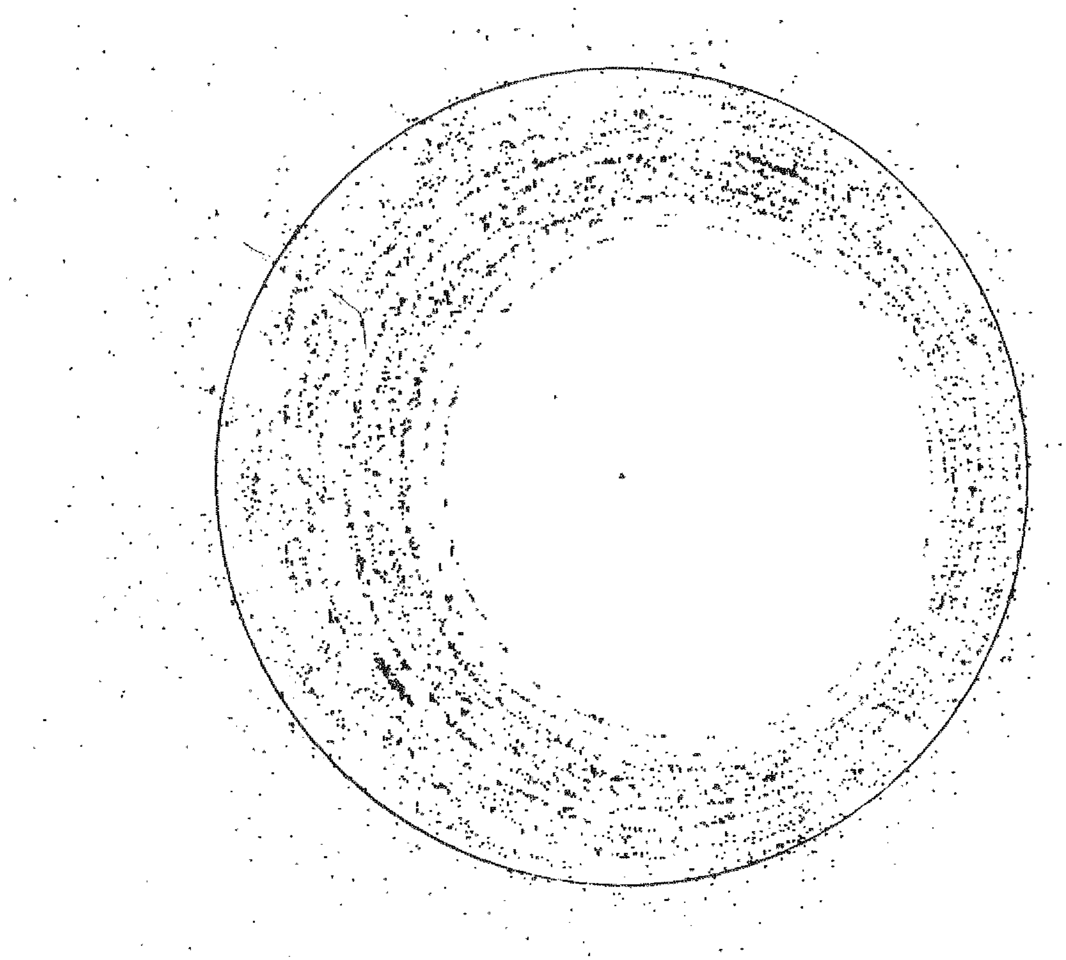

$$\beta_p = 1$$

$$\iota(a) = 0{,}276$$

$$\frac{I_{hel}}{B_\varphi} = 1\ \frac{kA}{T}$$

$$a_1 = 0.36$$

Fig. 15 135 field lines started in bundles of 45 each (cf. fig. 8), hower-ver near $\vartheta = 0$, 1 , 5. Each field line is traced 32 times around the torus.

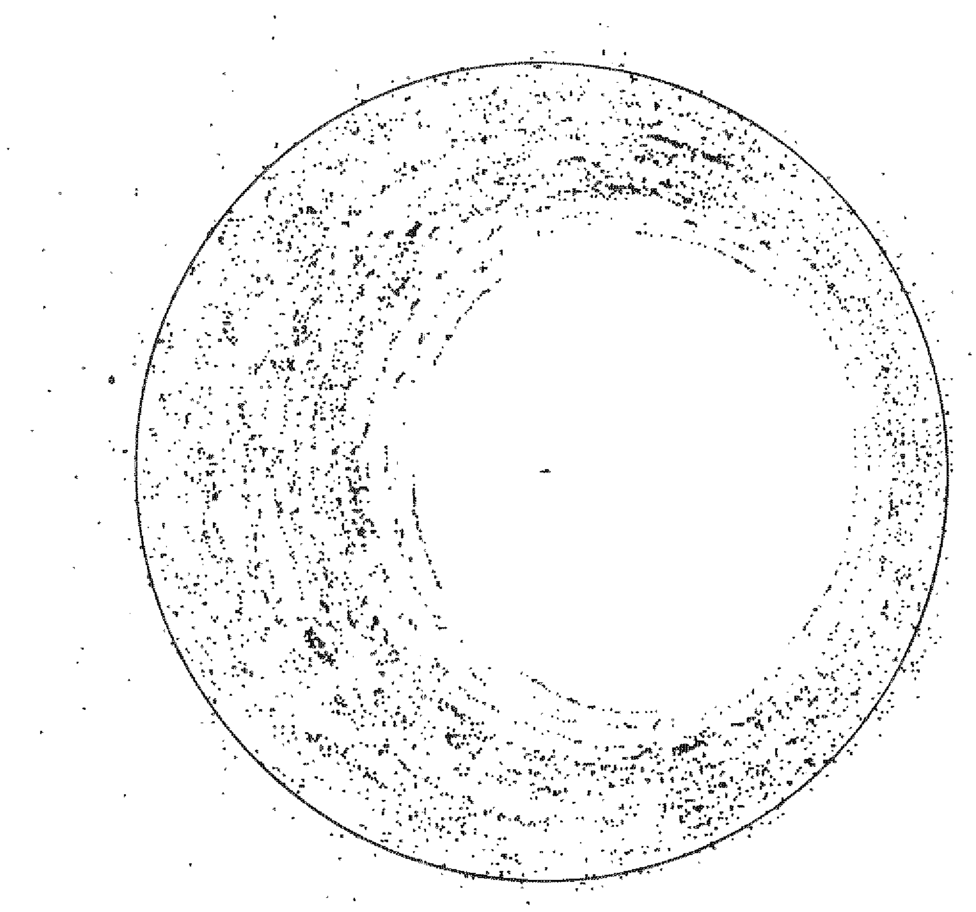

$\beta_p = 1{,}5$

$\iota(a) = 0{,}276$

$\frac{I_{hel}}{B_\varphi} = 1\ \frac{kA}{T}$

$a_1 = 0{,}36$

Fig. 16 135 field lines started.

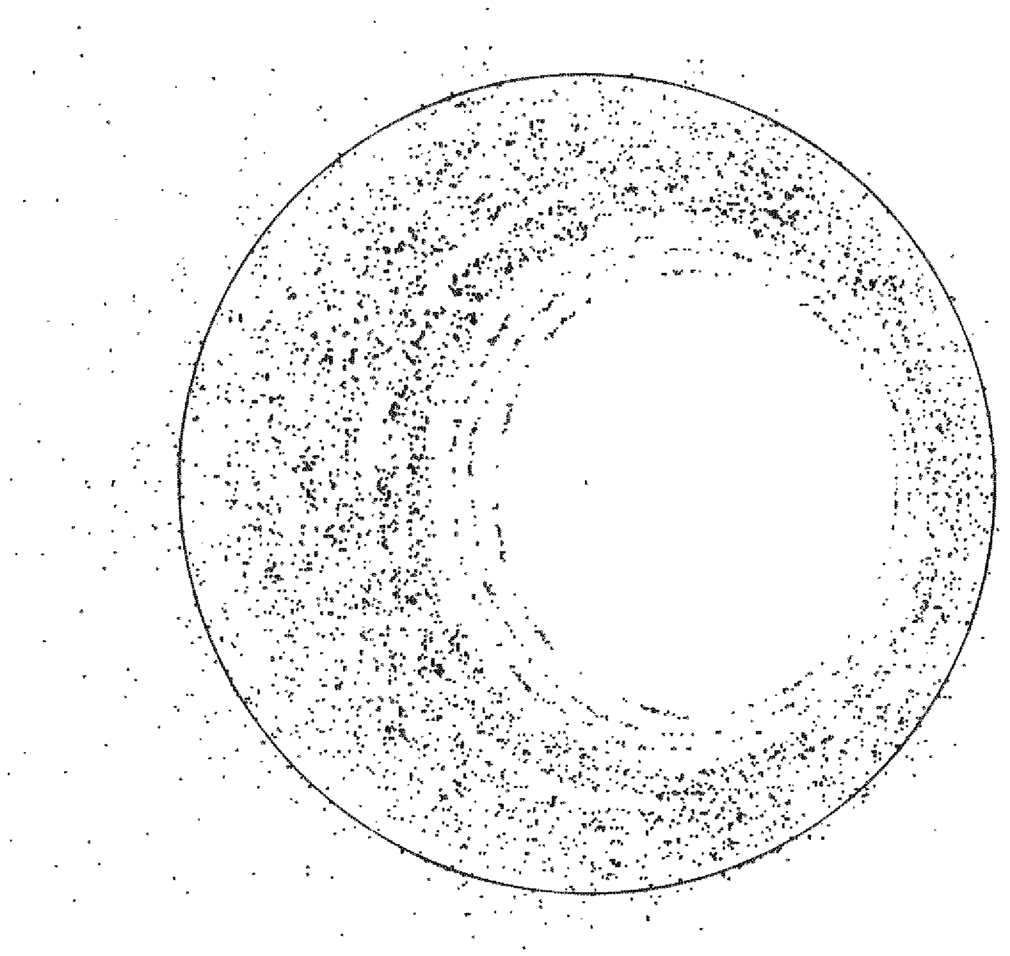

$\beta_p = 2$

$\iota(a) = 0{,}245$

$\dfrac{I_{hel}}{B_\varphi} = 1\ \dfrac{kA}{T}$

$a_1 = 0.36$

r_{start} = 82,5 cm
80 cm
77,5 cm
75 cm
72,5 cm
70 cm
67,5 cm
65 cm
62,5 cm

Fig. 17

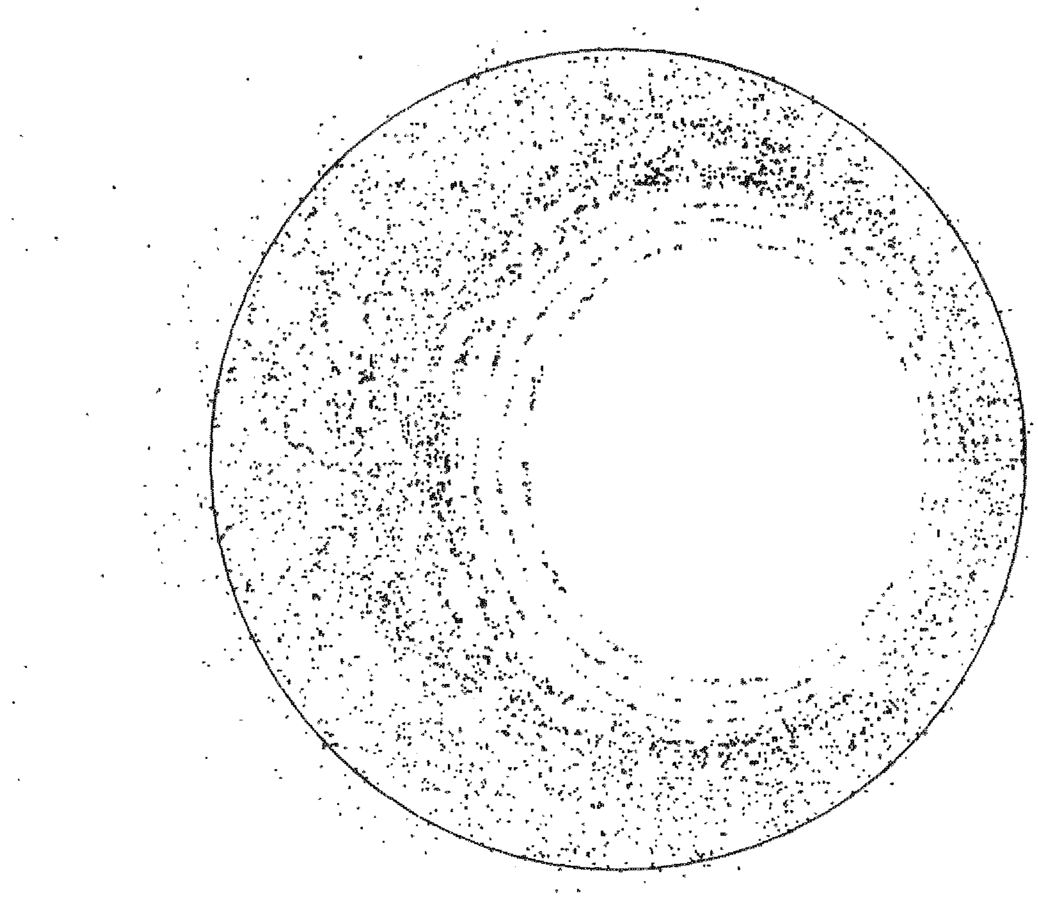

$\beta_p = 2$

$\iota(a) = 0{,}276$

$\frac{I_{hel}}{B_\varphi} = 1 \frac{kA}{T}$

$a_1 = 0{,}36$

Fig. 18

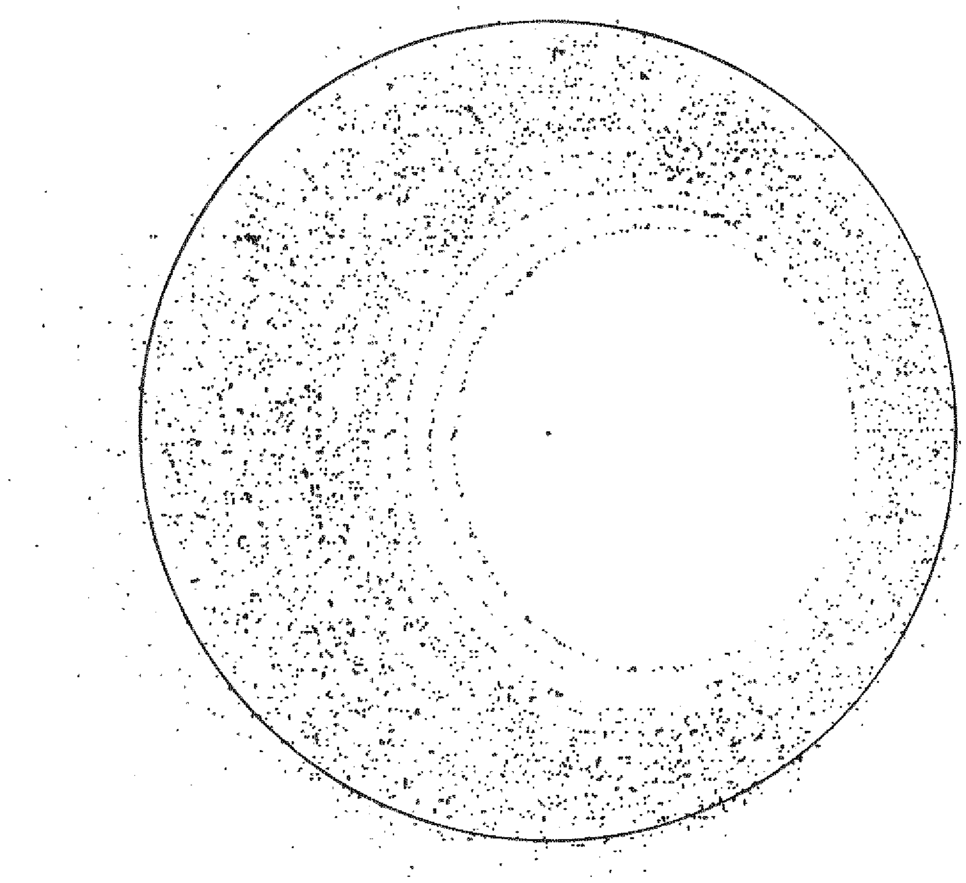

$\beta_p = 2$

$\iota(a) = 0{,}39$

$\frac{I_{hel}}{B_\varphi} = 1 \ \frac{kA}{T}$

$a_\iota = 0{,}36$

Fig. 19

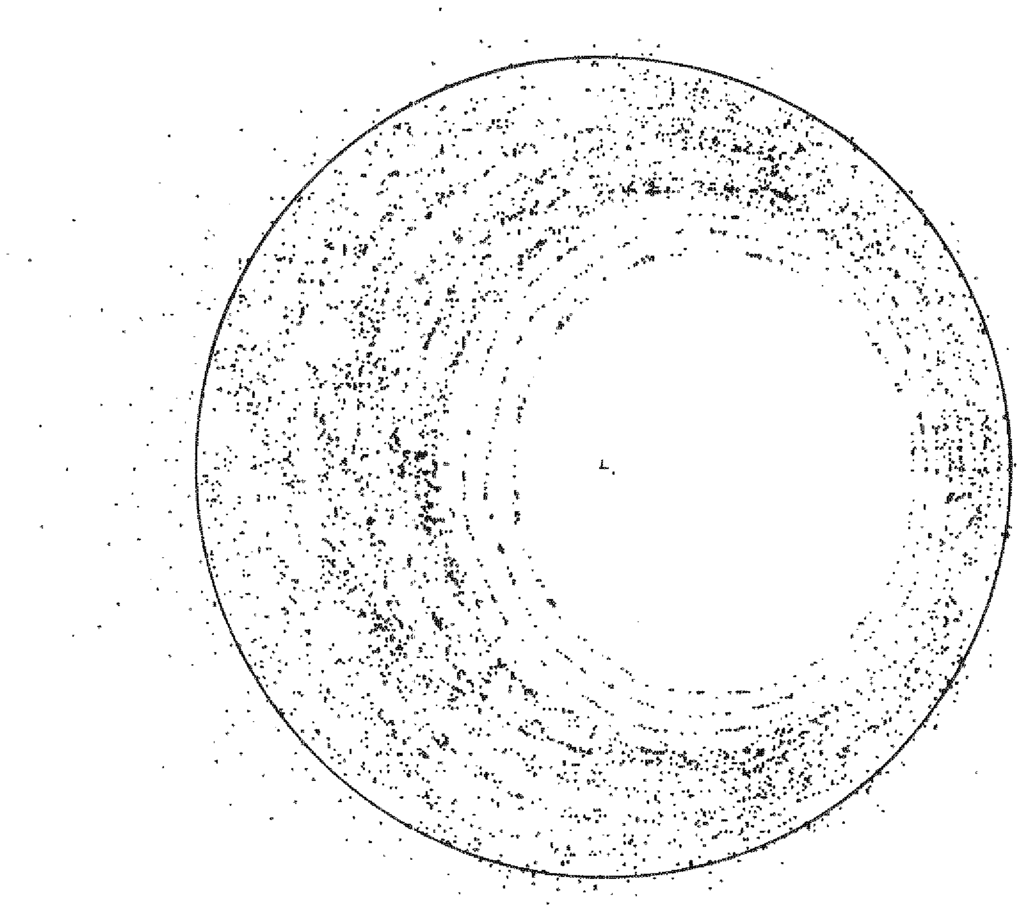

$\beta_p = 2$

$\iota(a) = 0{,}276$

$\dfrac{I_{hel}}{B_\varphi} = 1\ \dfrac{kA}{T}$

$a_1 = 0{,}46$

Fig. 20

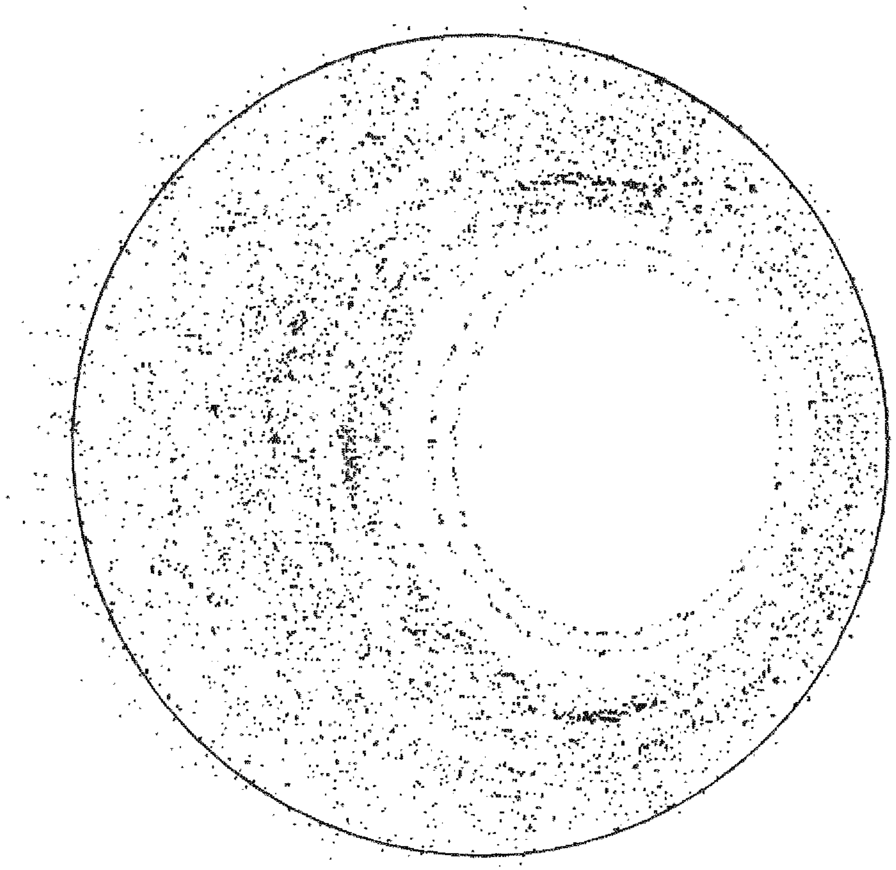

β_p = 2,5

$\iota(a)$ = 0,245

$\frac{I_{hel}}{B_\varphi}$ = 1 $\frac{kA}{T}$

a_1 = 0,36

r_{start} = 82,5 cm
80 cm
77,5 cm
75 cm
72,5 cm
70 cm
67,5 cm
65 cm
62,5 cm

Fig. 21 Same as fig. 21 for different β_{pol}

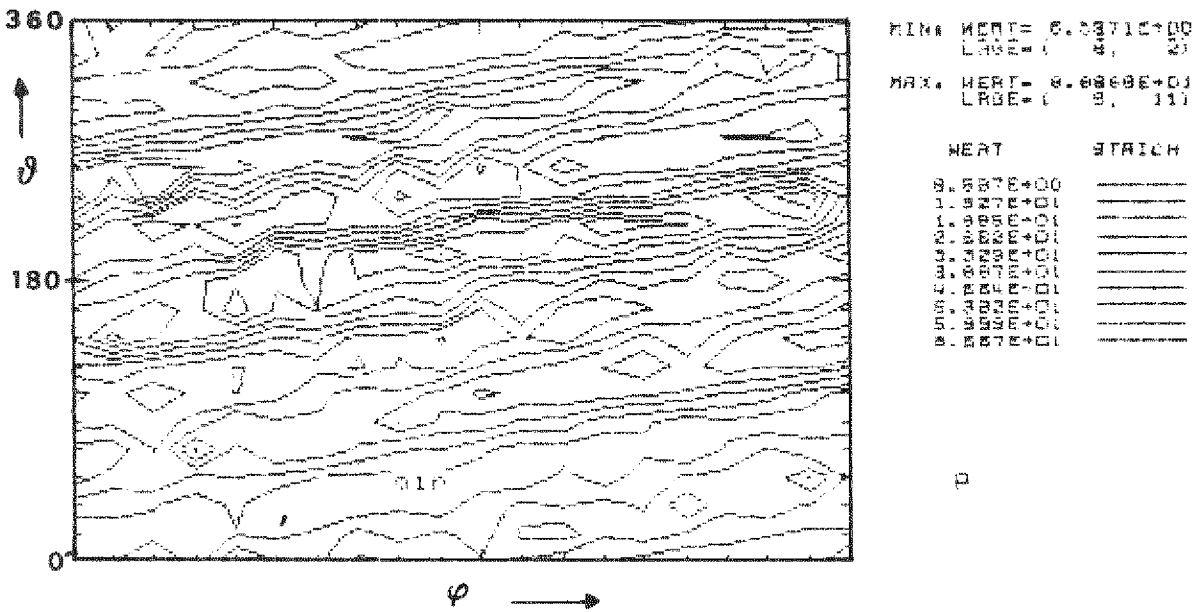

$$\frac{B_r}{B_\varphi} = 10^{-3}$$

$m = 4, \; n = 1$

$a = 50\,cm$

$q(42cm) = 4$

$r_{start} = 34\,cm$

Fig. 22 Density contour of field line intersection points with a toroidal surface as explained in the appendix. one minimum is indicated by min. The numbers (Wert) refer to the density (arbitrary units).

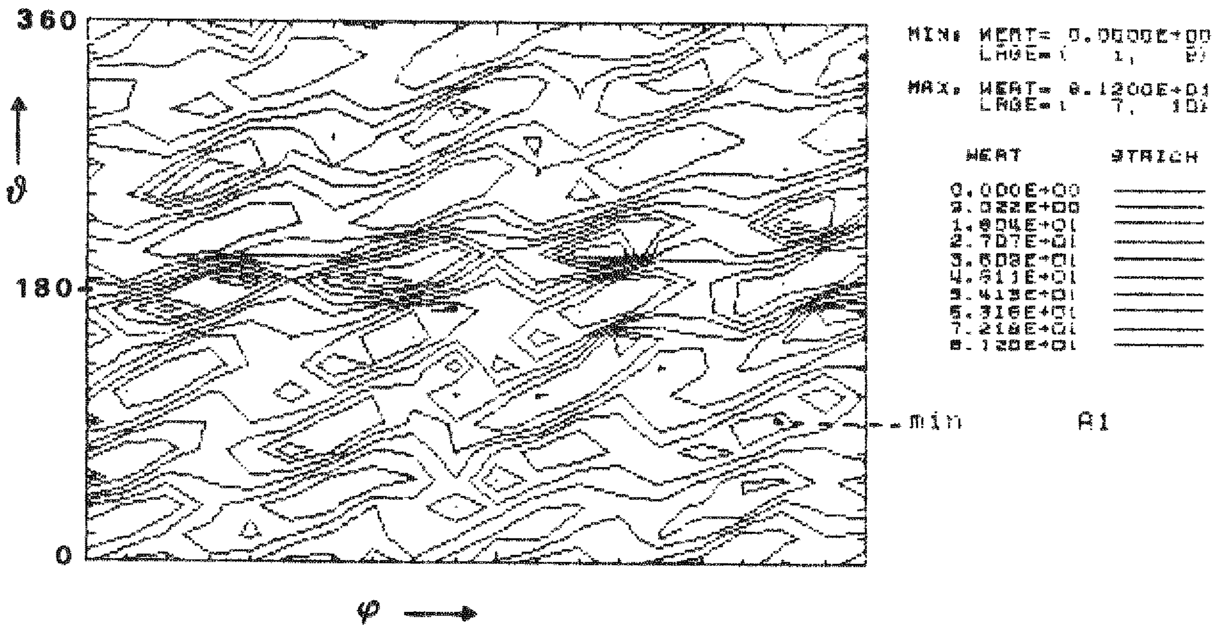

$$\frac{B_r}{B_\varphi} = 10^{-3}$$

$m = 5,\ n = 1$

$m = 4,\ n = 1$

$a = 50\,cm$

$q(42cm) = 4$

$r_{start} = 34\,cm$

Fig. 23 The same startconditions as in fig. 34, however, for different B_r and radius of collection.

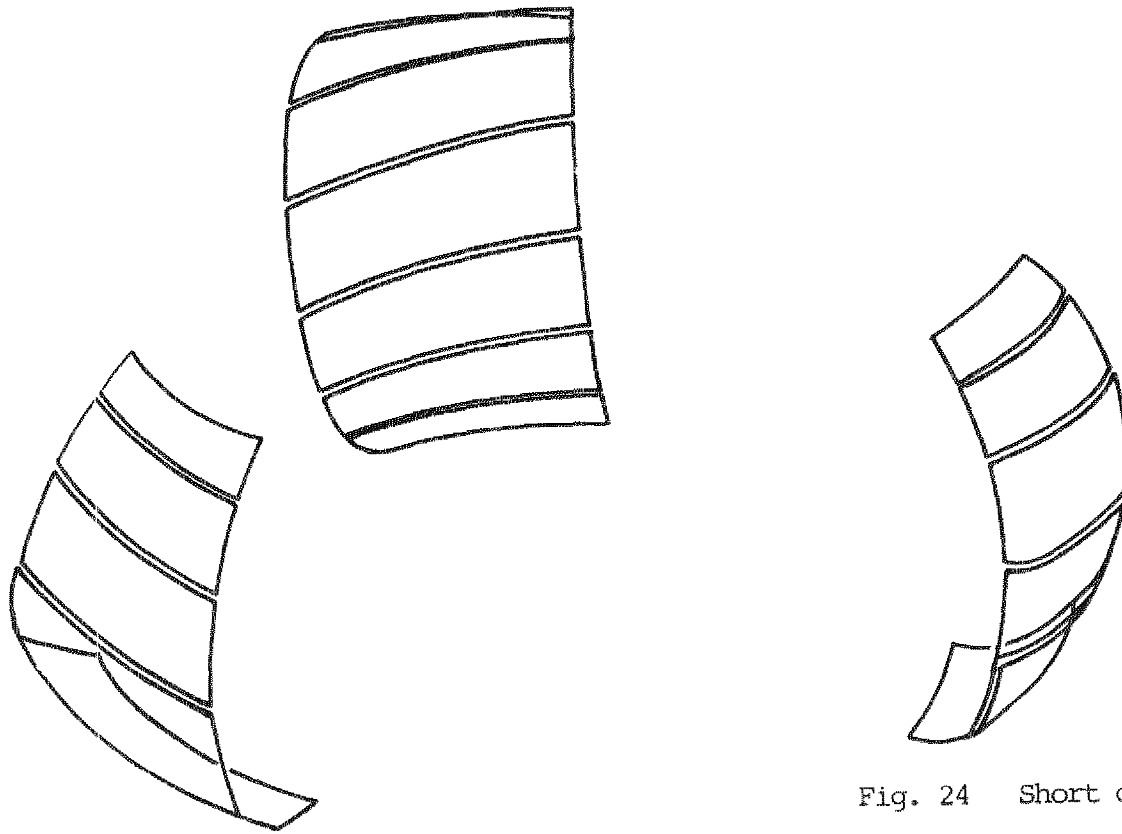

Fig. 24   Short coils (cf. Appendix)

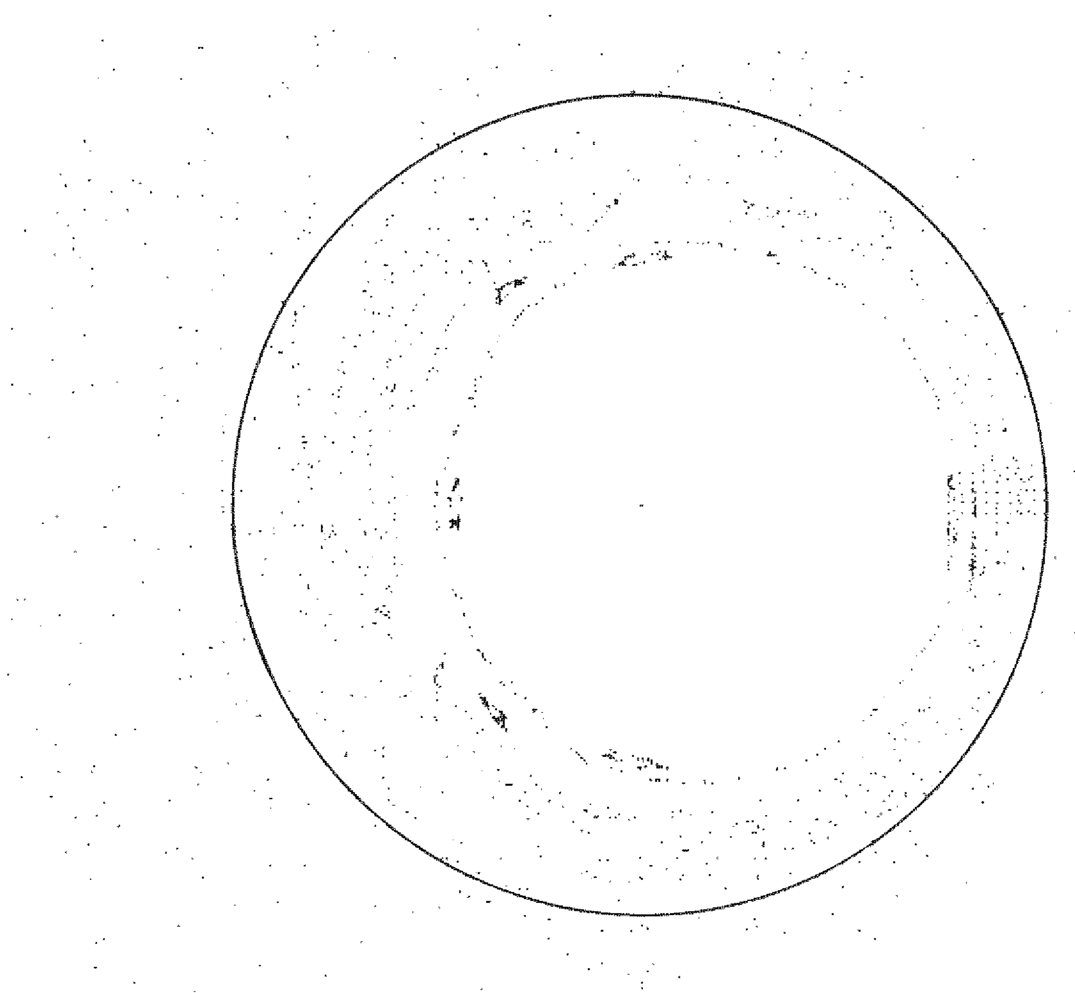

$$\beta_{pol} = 1$$

$$\iota(a) = 0{,}38$$

$$\frac{I_{hel}}{B_\varphi} = 3\ \frac{kA}{T}$$

$$a_1 = 0{,}33$$

Fig. 25 Poincaré plot for the disturbance caused by the short coils (fig 24)

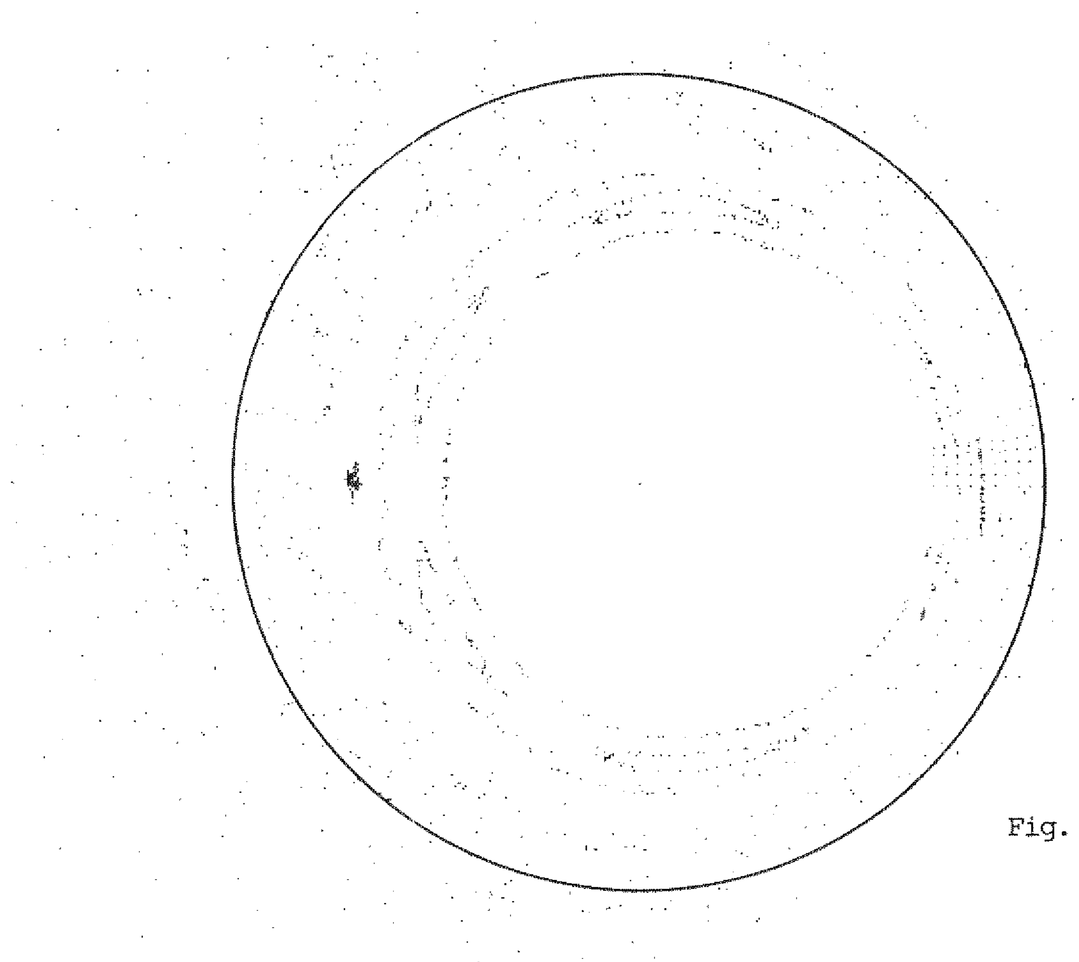

$$\beta_{pol} = 1$$

$$\iota(a) = 0{,}33$$

$$\frac{I_{hel}}{B_\varphi} = 2\ \frac{kA}{T}$$

$$a_1 = 0{,}33$$

Fig. 26   Same as fig. 25 for different